NASA CONTRACTOR REPORT

NASA CR-368

PROJECT FOG DROPS

INVESTIGATION OF WARM FOG PROPERTIES AND FOG MODIFICATION CONCEPTS

by Roland J. Pilié

Prepared under Contract No. NASr-156 *by*
CORNELL AERONAUTICAL LABORATORY, INC.
Buffalo, N. Y.
for

NATIONAL AERONAUTICS AND SPACE ADMINISTRATION • WASHINGTON, D. C. • JANUARY 1966

NASA CR-368

PROJECT FOG DROPS

INVESTIGATION OF WARM FOG PROPERTIES AND FOG MODIFICATION CONCEPTS

By Roland J. Pilié

Prepared under Contract No. NASr-156 by
CORNELL AERONAUTICAL LABORATORY, INC.
Buffalo, N.Y.

for

NATIONAL AERONAUTICS AND SPACE ADMINISTRATION

For sale by the Clearinghouse for Federal Scientific and Technical Information
Springfield, Virginia 22151 - Price $3.00

ABSTRACT

15317

Mathematical models have been formulated to describe the dynamic properties of warm fog. In the laboratory, experiments were conducted to determine the effects of ionic surfactants on droplet coalescence and to study the behavior of nuclei treated with fatty-alcohol monolayers. Daily measurements were made of the nuclei active at slight supersaturations characteristic of natural fog. The results of these measurements together with past analytical and experimental findings were used to generate new ideas for fog suppression and to evaluate previous concepts for altering warm fog. A climatological survey of fog frequency in the Continental United States describes those regions having frequent occurences of dense fog, i.e. fog that limits visual range to 1/4 mile or less.

Author

TABLE OF CONTENTS

LIST OF ILLUSTRATIONS

LIST OF ILLUSTRATIONS

LIST OF ILLUSTRATIONS

LIST OF TABLES

I. INTRODUCTION

The occurrence of fog in the vicinity of air terminals is one of the principal causes of disrupted flight operations. Poor visibility attending natural radiation and advection fogs frequently brings air transportation to a halt. In many instances the fog persists for several hours and occasionally for days before minimum landing conditions (operational limits of ILS) are met.

Logically, a number of investigators have utilized a variety of techniques in attempting to disperse natural fog. Only the dissipation of supercooled fog, however, has met with general success (Schaefer, 1946; aufm Kampe et al., 1957; Jiusto and Rogers, 1960). Efforts to modify "warm" fog have not been as encouraging and to date no practical method of warm fog dispersal has been achieved. The difficulty of this problem is usually attributed to the stability of the population of droplets comprising warm fog. Uniformity of droplet sizes discourages growth by coalescence and, hence, retards precipitation. Most investigators agree that the solution of the problem requires increased knowledge of the basic chemical, physical and electrical properties of fog.

Recognizing the need for additional research in this area of weather modification, the National Aeronautics and Space Administration has for the past two years contracted with the Cornell Aeronautical Laboratory to investigate basic fog and droplet properties together with possible methods of fog dispersal.

The first year's program emphasized work on:

1. Models of the micro- and macroscopic properties of warm fogs.

2. The characteristics of aerosol droplets and means of favorably altering these properties.

3. The construction of apparatus for simulating certain fog conditions.

4. Experimental alteration of the growth or evaporation rate of otherwise stable aerosol droplets.

5. Formulation of fog modification concepts based on the above findings, as well as a review of other possible techniques.

6. Assessment of the supercooled fog problem in the United States and specification of the geographic areas where an operational seeding program might be practical.

Accomplishments of that effort were discussed in the First Annual Summary Report. The accomplishments of the second year's effort are reported herein and are summarized in the next section. As illustrated by that summary the research to date has been very rewarding and productive, both in terms of new ideas for fog suppression and in terms of generating new information about the properties of fog and fog droplets.

II. SUMMARY OF PROGRAM ACCOMPLISHMENTS

1. Dynamic models have been formulated for advection, radiation and steam fog for various temperature, roughness and stability conditions. For each of the fog types, height distributions of temperature, liquid water content and visibility are given. These models have contributed significantly to our understanding of warm fog and the mechanisms that act to determine fog properties.

2. In the laboratory, ionic surfactants were found to substantially inhibit the coalescence of water droplets with a plane water surface. On the other hand, coalescence of treated 300μ radius drops colliding in air was not appreciably influenced by the presence of surfactant. It will be necessary to conduct experiments with colliding drops having sizes more nearly representative of natural fog (i.e. ~50μ diameter).

3. Surface treatment of sodium chloride crystals (a type of condensation nucleus found in the atmosphere) with hexadecanol and octadecanol was shown to substantially retard the growth rate of droplets formed on such nuclei. Nuclei could not, however, be prevented from participating in droplet growth except when impractically thick layers of surfactant were present.

4. Measurements were made of the drop size distributions in fogs occurring in the Buffalo area. Evaluated data were in good agreement with the values given by the physical fog models. In future observations, the measured average drop size is likely to be somewhat lower owing to a recent improvement in sampling technique designed to reduce preferential capture of larger drops.

5. A thermal diffusion chamber, designed and constructed on this program, was used to make daily measurements of the concentration of condensation nuclei at supersaturations characteristic of natural fog. An important conclusion of this investigation is that in urban fogs at least,the maximum supersaturation achieved is substantially less than 0.1%.

6. Results of nuclei concentration measurements at an urban site (near the Buffalo airport) and in a region relatively free of pollution (Springville, N. Y.) suggest that sources of atmospheric contaminants are not the major contributors to "fog nuclei" and that in the absence of local sources of such contaminants, sufficient nuclei are still available for droplet growth even at supersaturations of a few hundreths of one percent.

7. From a literary survey of past fog modification efforts and from the results of experiments conducted in our laboratory, three concepts for fog suppression have evolved and are being considered for further development on this program. In particular, we are considering methods for modifying the distribution of drop size in fog so that for a given liquid water content more large drops and fewer small drops exist. Such a procedure would result in a) increased precipitation rates and b) better visibility in fog. The first of these concepts involves retardation of diffusional growth of droplets by treatment with hexadecanol and octadecanol monolayers. Treated drops would not compete for available water thereby permitting untreated drops to grow to larger sizes. This concept was presented in the First Annual Summary Report NASA CR-72 and will not be discussed in detail here. The second method for fog suppression involves electrical charging of droplets positively and negatively in alternate adjacent regions of a fog to promote droplet coalescence. The last concept seeks to prevent the activation of most natural nuclei in fog by introducing a relatively small number of large, extremely hygroscopic nuclei into the air prior to fog formation. More detailed discussion of the last two concepts can be found in Section III, Part E, Numbers 2 and 3.

8. A detailed climatological survey of fog frequency in the U. S. indicates that warm fog constitutes a significant problem for aviation over 60% of the Continental United States. The survey defines the geographical regions of the United States where fog is most severe.

III. TECHNICAL DISCUSSION

A. Mathematical Fog Model*

One objective of the investigation of warm fog properties has been the development of representative models for the vertical distributions of temperature and liquid water in common types of fog. Such models are useful, first of all, in extending the limited present knowledge of these basic fog properties. Secondly, information derived from the models permits evaluation of the role of different physical mechanisms which contribute to fog formation. This information will be useful in assessing the potential of suggested fog modification techniques.

Detailed observations of temperature, visibility, and liquid water in fog are quite scarce. Therefore we have derived fog models from a basically theoretical viewpoint, using available data on gross fog properties and environmental conditions as a guide. The resulting models provide a useful description of typical fog characteristics and, in addition, indicate some of the physical relationships between fog properties and the environment. In this section examples of the fog models and the methods used in deriving them are presented.

---

*By George E. McVehil

1. Theoretical background

G. I. Taylor (1917) presented a graphical method for calculating the liquid water content produced by the mixing of two air masses of initially different temperatures. This method is illustrated in Figure 1. If the air masses are represented by A and B, respectively, the point C, lying on the line AB, represents the mixture. The position of C depends on the proportions of the two air masses. If C lies above the saturation line, the mixture is supersaturated and represents foggy air. Assuming that all of the excess water is condensed, the length of line CD then gives the amount of liquid water in the mixture.

Brunt (1935) pointed out that the latent heat released in the condensation process would heat the surrounding air-water vapor mixture. Therefore the resultant state E would be at a higher temperature than D. This means that the Taylor method systematically over-estimates the liquid water content. Brunt derived an expression for a correction factor representing the ratio of actual liquid water content to that which would be found by Taylor's method.

Recently Rodhe (1962) presented a mathematical fog model. Using the relations

$$H = -\rho\left[c_p + T'\frac{d}{dT'}\left(\frac{Lv'}{T'}\right)K_H\frac{\partial T'}{\partial z}\right]K_H\frac{\partial T'}{\partial z} \qquad (1)$$

$$E = -\rho K_E\frac{\partial r}{\partial z} \qquad (2)$$

where H = vertical eddy flux of heat (positive upwards)

E = vertical eddy flux of total water content

ρ = density of the air

c_p = specific heat of dry air at constant pressure

T' = wet bulb temperature

L = latent heat of condensation

v' = saturation mixing ratio

z = height above ground

K_H = turbulent exchange coefficient for heat

K_E = turbulent exchange coefficient for water

r = total water mixing ratio = $v' + \omega$

ω = liquid water content (or vapor deficit for unsaturated air)

he derived an equation for the rate of change of water content with respect to wet-bulb temperature:

$$\frac{dr}{dT'} = \frac{EK_H}{HK_E}\left[c_p + T'\frac{d}{dT'}\left(\frac{Lv'}{T'}\right)\right] \qquad (3)$$

Rodhe demonstrated that the wet-bulb potential temperature is a conservative property for turbulent mixing in the boundary layer. Likewise the total water content, liquid plus vapor, is assumed to be a conservative property. Thus, the eddy diffusion of heat and water content may be represented by equations (1) and (2) respectively, where E is the vertical transport of total water, and H is the transport of total heat, latent plus sensible. The equations hold whether the air is saturated or unsaturated, and whether or not evaporation and condensation of liquid droplets occur.

The quantity in brackets in equations (1) and (3) represents the specific heat of moist air. A small term accounting for the sensible heat of the water has been neglected. Since we will be dealing only with small height differences, the wet-bulb temperature will be used in place of wet-bulb potential temperature.

Equation (3) follows directly from (1) and (2) and represents a differential relation between wet-bulb temperature and total water content. It may be considered as simply a combination of the definitions of the turbulent exchange coefficients, K_H and K_E . The equation is useful in the present context because we know or can infer much about the behavior of E, H, K_E , and K_H in some fog situations. Specification of these quantities and the total temperature difference between fog base and top permits

calculation of the vertical profile of liquid water content. The liquid water content at a height where the temperature is T is given by

$$\omega = v_1' - v' + \int_{T_1'}^{T} \frac{EK_H}{HK_E}\left[c_p + T'\frac{d}{dT'}\left(\frac{Lv'}{T'}\right)\right]dT' \qquad (4)$$

where the subscript 1 refers to the lower fog boundary. The integral in equation (4) describes a curve similar to AB in Figure 1, but with slight curvature due to the latent heat term, which varies with temperature. As in Figure 1, the liquid water content is given by the difference $r - v'$, total water minus saturation mixing ratio.

Taylor, and later Brunt, considered the graphical approach as a means for determining the state produced by the mixing of two discrete masses of air. The position of the final state on the line AB was determined by the proportions of the two original masses. Rodhe's formulation, on the other hand, aims at describing the continuous distributions of T' and r produced by turbulent exchange between two given levels. Thus, we now consider each point on AB (actually the curved modification of AB given by equation (4)) to represent the state at a different height in the boundary layer; the end points represent the ground surface and some level above the fog top. It is assumed that the liquid water content at the surface is always zero. Thus, in the presence of fog the surface is always wet, evaporation or condensation is taking place, and the water content of the air at the surface is just equal to the saturation vapor content at the surface temperature.

Equation (4) has been used to derive the fog models to be presented here. The calculation of liquid water profiles requires specification of the factor EK_H/HK_E , so that the integration in equation (4) can be performed, and the relationship between temperature and height, so that the derived $\omega - T$ relationship may be transformed into an ω vs. z curve.

Two distinct classes of fog have been modelled, the difference depending upon the assumption that is made concerning the ratio E/H. (The ratio K_H/K_E is determined by the choice of temperature and total water profiles - it will always be taken as unity in what follows.) If we assume that E and H are constant both with time and height, the fog would be classified as a pure advection fog. We imagine an air mass with given properties moving over a wet surface of temperature different from the air. With E and H constant, there is a constant flux of heat and moisture through the boundary layer and time changes of temperature and moisture content are zero. The distribution of temperature and moisture is determined purely by the turbulent mixing. Figure 2 illustrates this situation. Point A represents the surface condition, point B the condition in the airmass above the fog top. Curve AB is an integral of equation (4) for constant E/H. It gives the relationship between T' and r through the boundary layer. It is seen that fog will exist from the surface to near the height of point B, due to the curvature of the saturation line, which is greater than that of the line AB. However, it is also clear that only modest liquid water content can be produced in this way, and any appreciable liquid water content requires a large temperature difference between the fog base and top.

In order to account for the larger of observed liquid water contents, it is necessary to relax the restrictions on the behavior of the heat and water transports. If we permit E/H to change with height, we have the case of radiation fog, or more properly, mixed advection-radiation fog. (Since our model is based upon the laws of turbulent mixing, we require some turbulence, which is certainly present in the vast majority of all natural fogs.) Where radiational cooling of the air and fog droplets occur, temperature changes alter the form of the temperature profile. Turbulence then acts to balance the radiational heat losses; the result is a convergence of turbulent heat flux in the region of radiative heat loss. The vertical eddy heat flux, H thus changes with height. There is no corresponding reason to expect variations in E, and so the ratio E/H varies in the vertical. The radiation fog curve in Figure 2 shows a typical result when these changes of E/H are

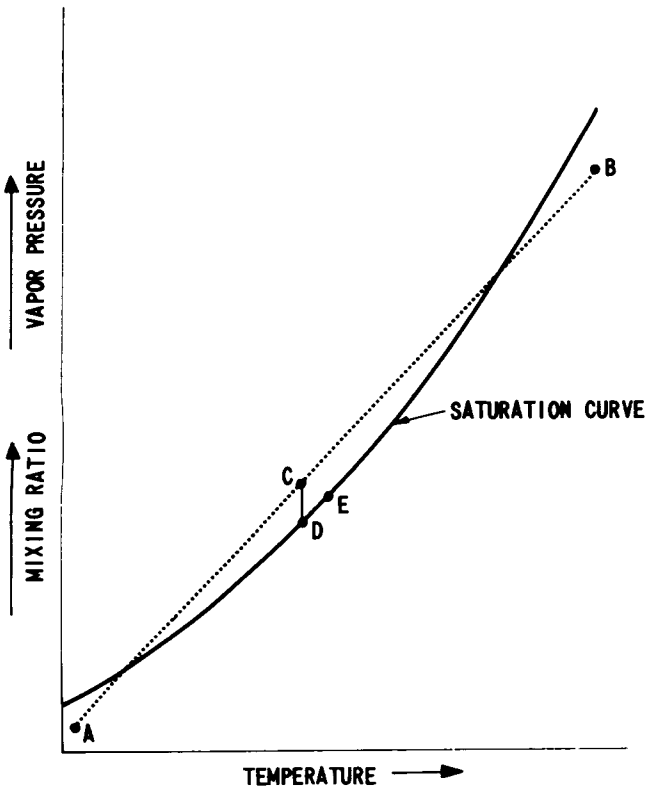

Figure 1 TAYLOR GRAPHICAL METHOD FOR CALCULATING LIQUID WATER CONTENT

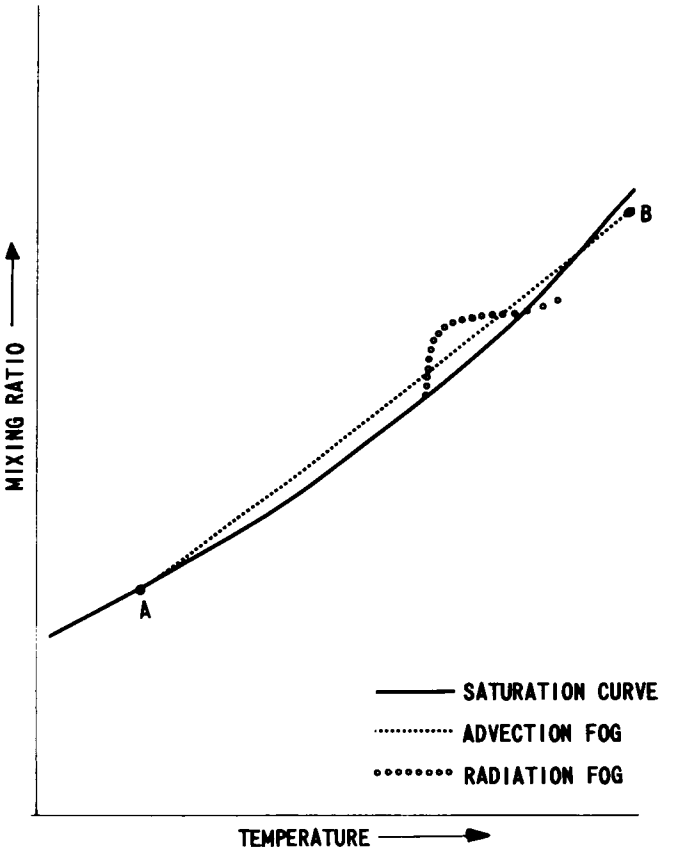

Figure 2 ADVECTION AND RADIATION FOG CASES ON TEMPERATURE MIXING RATIO DIAGRAM

included in the evaluation of equation (4). Note that though the temperature difference through the fog is less than 3 deg. C, supersaturations well in excess of those in advection fog result.

2. Calculation of Fog Models

Advection fog

So long as EK_H/HK_E is taken as constant, there is no difference in theory between the Taylor-Brunt graphical method and the Rodhe equations for computing liquid water content. Approximations introduced by the numerical integration or graphical techniques will, however, result in small differences between the two results. A comparison between the Taylor-Brunt and Rodhe techniques has been made and it was found that the differences were negligible except for extreme cases where the temperature difference between fog base and top was 20 degrees C or more. Therefore, the simpler Taylor-Brunt method has been used for determining the amount of liquid water for all advection fog models.

Curves showing the relationship between temperature and liquid water content were drawn for a variety of surface temperatures and temperature differences between fog base and top. These relationships were then used with selected vertical temperature profiles to derive the advection fog models.

Radiation fog

The vertical distribution of radiative heat flux is required for evaluation of equation (4) in the case of radiation fog. Radiative flux divergence was calculated for two fog depths and densities using simplified radiative transfer equations. It was assumed for the radiation calculations that the liquid water content was constant and that the temperature increased linearly from fog base to top. The downward radiation from the atmosphere above the fog was neglected. The resulting profiles of radiative flux divergence showed an increase of divergence (cooling rate) with height, as would be expected. The radiation model, though crude, provided estimates of the

distribution of flux divergence which are felt to be adequate for demonstrating the role of radiation in determining fog properties.

It was assumed that the turbulent heat flux divergence exactly balanced the radiative flux divergence calculated as discussed above. The radiation fog temperature profiles were then computed on the basis of these heat flux profiles by the method discussed in part 3.

The liquid water content for radiation fog was computed by numerical integration of equation (4). Fog base and top temperatures of +5 deg. C and +10 deg. C, respectively, were used for both calculated cases. The necessary values of H as a function of temperature were taken from the vertical profiles of H and T derived as above. The value of E, not a function of height or temperature, was chosen so as to make the water content go to zero at the preassigned fog top.

3. Temperature Profiles

There have been few systematic studies of temperature profiles through fog. Most analytical fog investigations have assumed temperature distributions chosen more for mathematical convenience than for realism. A logarithmic profile, often used to represent wind and temperature distributions in the boundary layer, is quite realistic for near-adiabatic conditions but since most fog cases occur in extreme temperature gradients, both stable and unstable, more general profile relationships are needed.

The profiles adopted for the present study are based on the widely accepted similarity analysis of Monin and Obukhov (1954). A general view of the results of this approach is given by Lumley and Panofsky (1964). Applications and comparisons with observations have been given by Panofsky et al. (1960) and McVehil (1964). The theory describes the profiles of wind and temperature and is outlined here initially with reference to horizontal wind speed.

A normalized vertical wind shear can be defined by

$$S = \frac{kz}{u_*} \frac{\partial u}{\partial z} \tag{5}$$

where k is von Karman's constant, 0.40, u is the mean wind speed, and u_* is the "friction velocity" given by $(\tau/\rho)^{1/2}$ with τ the horizontal shearing stress. S is a dimensionless characteristic of the wind profile, equal to unity in neutral stratification. Monin and Obukhov defined a stability parameter with dimensions of length by

$$L = - \frac{u_*^3 c_p \rho T}{k g H} \tag{6}$$

For non-neutral conditions, they concluded from dimensional analysis that

$$S = \phi\left(\frac{z}{L}\right) \tag{7}$$

where ϕ is an unknown function. They suggested as a first approximation expanding ϕ in a power series and using the linear term only. Thus

$$S = 1 + \alpha \frac{z}{L} \tag{8}$$

where α is some constant. Integration of equation (8) leads to what is called the "log + linear" wind profile

$$u = \frac{u_*}{k}\left(\ln \frac{z}{z_o} + \alpha \frac{z - z_o}{L}\right) \tag{9}$$

(Recall that u_* is assumed to be constant in the boundary layer.) z_o is the roughness length, the height at which $u = 0$.

The log + linear equation has been found to be generally applicable in stable conditions (McVehil, 1964). In unstable conditions, it is valid only over a limited range of z/L . A better expression for ϕ in unstable air is (Panofsky, Blackadar, and McVehil, 1960)

$$S^4 + \gamma \frac{z}{L} S^3 = 1 \tag{10}$$

where γ is another constant, equal to about 14. The wind profile for the unstable case may be derived from equation (10) by numerical integration.

The turbulent exchange coefficient for momentum is expressed in the present notation as

$$K_M = \frac{u_*^2}{\partial u / \partial z} = \frac{kzu_*}{S} \tag{11}$$

Expressions for boundary layer temperature profiles corresponding to the above wind profiles can be derived by specifying a relationship between K_M and K_H . The general consensus at present is that K_H and K_M are nearly equal in most circumstances, or at least are in a constant ratio one to another. They have been assumed to be equal in the present analysis. It thus follows that the temperature profiles are given by

$$T - T_o = - \frac{H}{c_p \rho u_* k} \left(\ln \frac{z}{z_o} + \alpha \frac{z - z_o}{L} \right) \tag{12}$$

for stable stratification (inversion), and

$$T - T_o = - \frac{H}{c_p \rho u_* k} \int_{z_o}^{z} S \, d \ln z \tag{13}$$

for unstable conditions. In both equations, T_o represents the temperature at $z = z_o$. For integration of equation (13), S is taken as the function of z/L defined by equation (10).

The procedure applied in calculating temperature profiles for the fog models was to specify the surface temperature T_0, the height of the fog h, the total temperature difference through the fog $T_h - T_0$, the surface roughness z_0 and the stability length L. These quantities are all mathematically independent within the present framework. Their specification, along with the definition given by equation (6) and equation (12) or (13), determines all other unknowns and permits the calculation of the temperature profile. Alternately, one could omit specification of L and fix the wind speed at a given height, thus determining L through equation (9) or equation (10). The calculations were simplified in the present examples by making an a priori choice of L. Corresponding wind speeds for a height of 10 m were subsequently calculated and these are all realistic for the types of fog modeled. The choices of temperature, temperature difference, roughness, etc. were made with the objectives of depicting representative conditions in natural fogs, and demonstrating the effect of varying parameters on the fog properties.

For the radiation fog cases, it was necessary to derive temperature profiles for which the turbulent heat flux varied with height. The preceding equations all assume constant flux. There is no generally accepted theory for the temperature distribution under the combined influence of turbulence and radiation, but a generalization of the above equations was derived for use in the radiation fogs. We assume that the turbulent exchange coefficient is identical to that in the constant flux inversion cases, i.e.,

$$K_H = \frac{k z u_*}{1 + \alpha (z/L)}$$

where L is the value appropriate to the surface heat flux and stress. Then, retaining the usual relation between heat flux and gradient, the temperature profile is given by

$$T - T_0 = -\frac{1}{k u_* c_p \rho} \int_{z_0}^{z} H \left(1 + \alpha \frac{z}{L}\right) d \ln z \qquad (14)$$

Equation (14) was utilized in deriving the radiation fog temperature profiles. The integration was performed numerically, using an assumed value of L and the heat flux profile required to balance the calculated radiative flux divergence.

In all temperature computations, no account was taken of adiabatic temperature changes with height or of the effect of latent heat of condensation. In principle, the temperature-heat flux relationship should be that given by equation (1), with T' equal to wet-bulb potential temperature. The neglect of these two factors in calculating the temperature profiles produces a small distortion in the height distributions, but no significant effect on the general shape of the liquid water curves. The latent heat terms were of course included in calculating liquid water content.

4. Discussion of Results

Figures 3 through 12 show models of advection, radiation and steam fogs for a variety of temperature, roughness, and stability conditions. In each figure, three curves are given. These show the height distribution of temperature, liquid water content, and horizontal visibility in each type of fog. The visibility was computed by Trabert's formula (Mason, 1957),

$$V = 2.6 \frac{\rho \bar{R}}{\omega}$$

where $\bar{R}$ is the average drop radius, $1 \leq \rho \leq 2$ depending on the drop size distribution, and ω is liquid water content. The drop radius was taken as 5μ for radiation fog and 10μ for all others; ρ was taken as 1.5.

Looking first at the pure advection fogs, Figures 3 through 8, all water content profiles show the same general shape, with zero liquid water at top and bottom, and a maximum somewhere near the middle of the fog layer. The maximum value of liquid water attained in the fog depends only on the total temperature difference (ΔT) and the surface temperature, T_o. The effect of surface temperature is small in the range of practical interest (the maximum ω increases by less than 4% with a 5 deg. C increase in surface

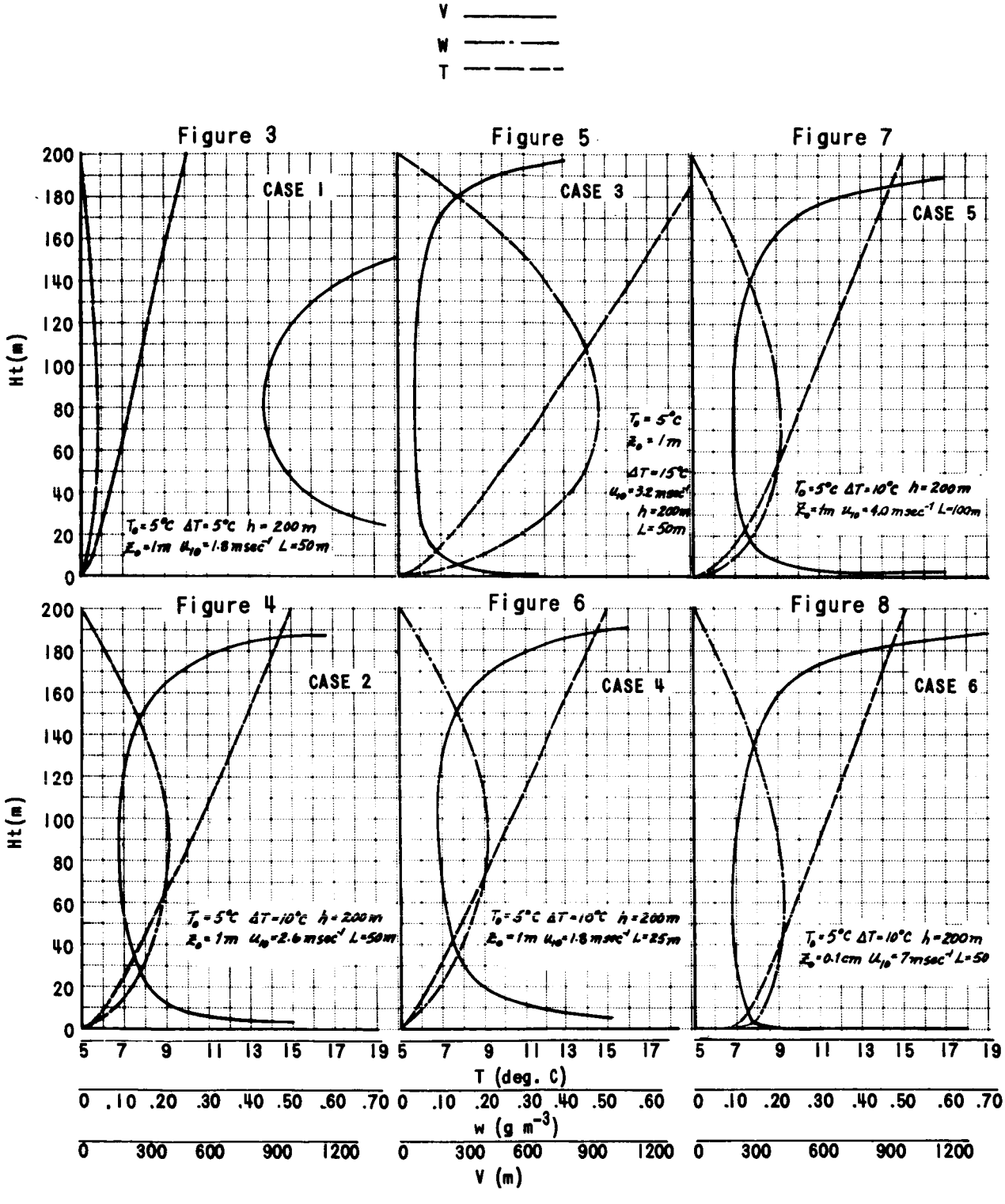

MODEL ADVECTION FOG

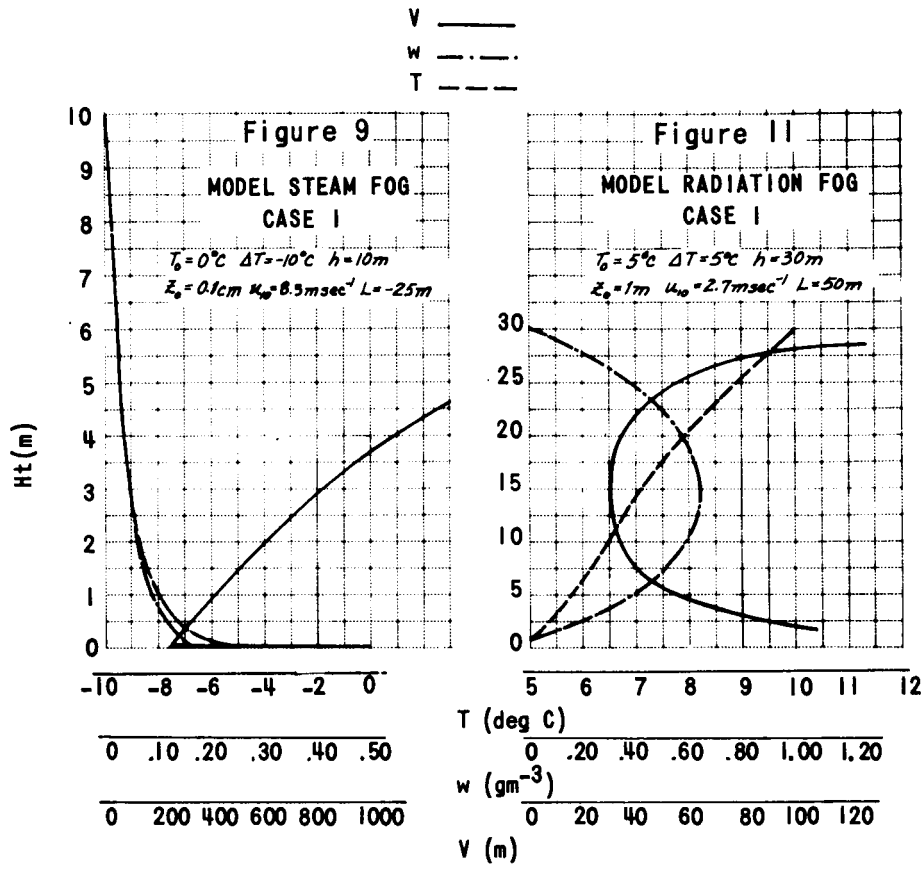
V
w
T
Figure 9
MODEL STEAM FOG
CASE 1
$T_0 = 0°C$ $\Delta T = -10°C$ $h = 10m$
$z_0 = 0.1cm$ $u_{10} = 8.5 msec^{-1}$ $L = -25m$
Figure 11
MODEL RADIATION FOG
CASE 1
$T_0 = 5°C$ $\Delta T = 5°C$ $h = 30m$
$z_0 = 1m$ $u_{10} = 2.7 msec^{-1}$ $L = 50m$
Ht(m)
T (deg C)
w (gm^{-3})
V (m)

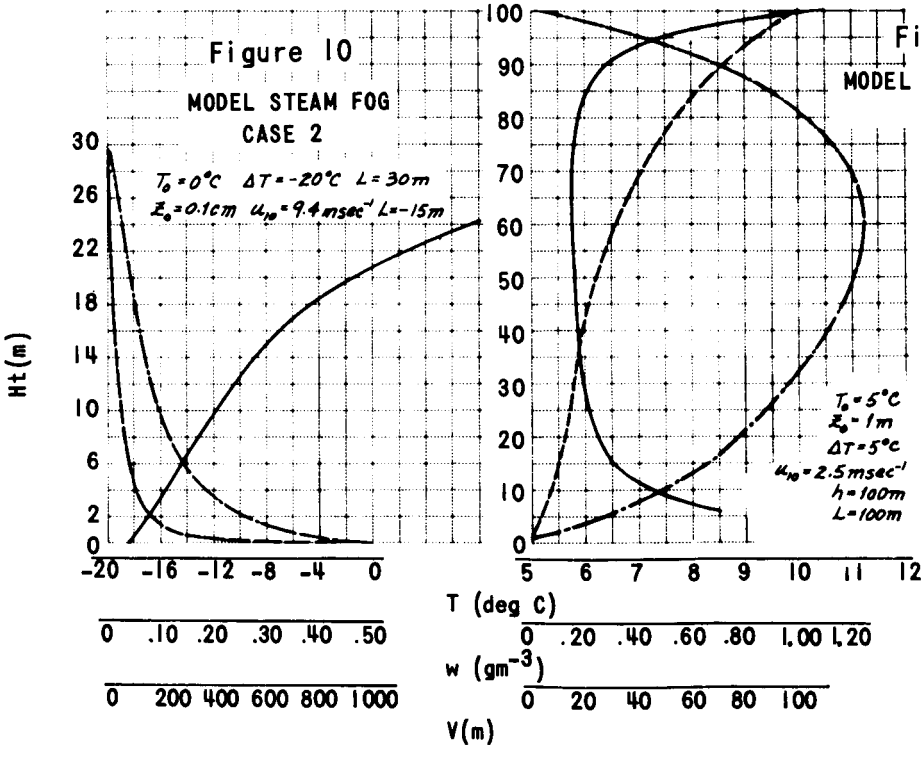
Figure 10
MODEL STEAM FOG
CASE 2
$T_0 = 0°C$ $\Delta T = -20°C$ $L = 30m$
$z_0 = 0.1cm$ $u_{10} = 9.4 msec^{-1}$ $L = -15m$
Figure 12
MODEL RADIATION FOG
CASE 2
$T_0 = 5°C$
$z_0 = 1m$
$\Delta T = 5°C$
$u_{10} = 2.5 msec^{-1}$
$h = 100m$
$L = 100m$
Ht(m)
T (deg C)
w (gm^{-3})
V(m)

temperature) and thus all models shown are for a surface temperature of 5 deg. C.

Figures 3, 4, and 5 represent advection fogs over identical surfaces but with increasing vertical temperature gradients. With ΔT = 5 deg, the maximum ω is only 0.045 g m^{-3} and the minimum visibility over 800 m. As ΔT increases to 10 deg. (Figure 4) and 15 deg. (Figure 5), ω at the maximum increases to 0.21 and 0.48 g m^{-3}, respectively. The crucial role of ΔT in determining the liquid water content is thus illustrated in these three figures. The hydrostatic stability was maintained constant in the three cases with a stability length of 50 m for each. Due to the increasing temperature gradient, this implies a corresponding increase in wind from Figure 3 through Figure 5, as indicated in the captions. An L value of 50 m represents a moderately stable situation and the combinations of wind and temperature difference represented by the models are felt to be realistic for advection fog.

It should be noted that in all cases the maximum water content occurs somewhat below the geometric center of the fog. The maximum is always found near the mid-temperature in the interval but due to the shape of the temperature profiles, with steepest gradients near the ground, this mid-temperature is always below the 100 m level.

The surface roughness was taken as 1 m for cases 3, 4, and 5. Such a value can be considered representative of level terrain with a cover of moderate sized trees, buildings, and open areas. A sea surface, for comparison, has a representative roughness length of about 0.1 cm (Figure 8).

Figures 6 and 7 show the effect of changing stability, with values of L equal to 25 and 100 m, respectively. The smaller value of L corresponds to greater stability, or a lighter wind for the same temperature difference and roughness. These figures should be compared to Figure 4, for which all parameters except L are identical. It can be seen that the stability effect is fairly small, acting only to skew the distribution of water content somewhat up or down. Greater stability (Figure 6) results in lower water content and better visibility near the ground with correspondingly more water near the top. The reverse is evidenced in Figure 7 where higher wind has been postulated

to give more nearly neutral stability. The effect is easily understood by considering the action of higher wind in producing more vertical mixing. More intense mixing (between the fixed boundary temperatures that we have assumed) results in a steeper temperature gradient near the ground so that high temperatures (and greater liquid water) are shifted toward the lower boundary.

Figure 8, in comparison with Figure 4, demonstrates the influence of surface roughness. The conditions for Figure 8 are identical to those in Figure 4 except that the roughness has been reduced to 0.1 cm. This example should represent fog over the ocean, as opposed to the others which are appropriate to an advection fog forming or carried over land areas. The effect of the smaller roughness is to shift the water content to lower altitudes. The smoother surface produces less mechanical turbulence near the ground and a much larger percentage of the total temperature change in the lowest few meters therefore resulting in a concentration of the water at these levels. The roughness effect probably explains in part why the densest fogs (at observation level) are normally observed at sea.

Steam fog models are shown in Figures 9 and 10. The former represents a temperature difference of 10 deg between water and fog top, the latter a difference of 20 deg. Fog heights have been assumed to be 10 and 30 m, respectively. The difference in liquid water profiles between these and the warm air advection fogs is striking. Note that the liquid water content does go to zero at the surface in the steam fogs, but the maximum liquid water content occurs at such a low level (below 20 cm) that for practical purposes the fog can be considered to decrease in density with height upward from the surface. The low roughness over water in part produces the concentration of liquid water content near the surface, but the main reason for this is the different shape of the temperature profile in unstable air. The temperature change is almost entirely concentrated into the lowest meter, and so nearly all of the fog occurs there. As stability increases the profile approaches a linear form. With decreasing stability, the profile becomes more curved, with more and more of the gradient concentrated near the surface. Thus the

characteristics of the temperature distribution rather than the physics of the fog formation are responsible for the great difference between advection and steam fog liquid water distributions.

Radiation fog results are shown in Figures 11 and 12. The first is for a 30 m fog depth and the second for a 100 m depth. The stability was taken to be somewhat greater in the shallower fog, due to the greater vertical temperature gradient. The primary difference between the two cases is in the radiation profiles. With the thicker fog, the turbulent heat flux must undergo larger changes to balance the radiation losses, and the resulting distortion of the temperature profile permits considerably greater liquid water content to be attained.

The two radiation fogs show generally similar liquid water profile shapes. Note that the maximum liquid water in the radiation fog tends to be found near or above the middle of the fog, whereas for the advection fogs it was usually below. This result is a consequence of the steep temperature gradient in the upper half of radiation fog, which is in turn a result of the radiational heat losses from the fog top.

The calculated liquid water contents in radiation fog are higher than generally accepted values. The primary reason for this is believed to be the neglect of downward sky radiation in the radiation calculations. In most actual cases, the radiational heat losses would be reduced from the values used in our calculations with a consequent reduction in observed liquid water content.

Radiation fog examples for other combinations of parameters have not been derived. The necessarily approximate treatments of radiative transfer and temperature distribution used in the models do not justify the detailed examination of wind speed, roughness, and stability effects as in the advection models. Qualitatively, these variables will influence a radiation fog in the same manner as an advection fog, but the magnitude of the effect will usually be less, since the radiation itself has the primary influence on fog properties.

Several factors should be kept in mind in interpreting all of the fog models. The assumed boundary conditions are fixed, and are taken as independent of the fog itself. In addition, the fog models apply to equilibrium states with zero time rates of change. In actual fogs, true equilibrium probably is seldom reached and boundary conditions may change with time. In radiation fog especially, time changes are likely to be important as the fog grows and temperatures both aloft and at the ground change. Liquid water profiles observed in fog should be expected to be less uniform than those derived here, and in particular cases to differ substantially.

The primary usefulness of the present models should be in showing the manner in which the thermo- and hydrodynamical processes act to determine the fog properties. The models should not be considered detailed representations of actual fog distributions. Refinement of these models and more accurate quantitative predictions of fog characteristics can be achieved when observations are available for comparison.

B. Laboratory Droplet Growth Experiments*

1. Coalescence studies with surfactants

Surfactants typically consist of long organic molecules that are said to be amphipathic, i.e. different parts of the molecule show very different behavior relative to a solvent. If the solvent is water, one end of the surfactant molecule is hydrophylic and the other hydrophobic. When in contact with water the hydrophylic end of the molecule buries itself in the liquid water while the hydrophobic part (hydrocarbon) projects into the gas phase above the interface. Since the concentration of the surfactant at the surface is much greater than in the liquid a monomolecular film is produced over the water surface.

Ionic surfactants have the additional property of separating into oppositely charged ions when dissolved in water. For the most part, the predominantly organic portion of the molecule becomes concentrated at the interface, carrying with it the anionic or cationic portion of the molecule to produce a charged layer at the water surface. The counter ion, consisting of a charged atom or small group of atoms, is distributed throughout the bulk of the water. Anionic surfactants produce a negative charge layer at the interface and cationic surfactants a positive one. For example, an anionic surfactant, sodium heptadecyl sulfate, will produce a negative surface active ion and thus a negative surface charge layer. Na^+, the counter ion, becomes distributed throughout the remainder of the liquid water. The net charge of the drop is not altered by the presence of the surfactant.

It has been suggested by several investigators that treating water droplets with certain ionic surfactants might increase their coalescence rates or perhaps influence their diffusional rate of growth. Elton (1958) has postulated the use of ionic surfactants as a possible means of altering droplet

*By Warren C. Kocmond

surface charge in some fogs. Benton et al., (1958) suggested that the coalescence of droplets might be enhanced by selective treatment of droplets with surface active agents. On the other hand, Lieberman (1960) reports that laboratory produced fogs tend to stabilize when treated with ionic surfactants rather than to dissipate. Field tests conducted by the Air Force in Arcata, California indicate that surfactants do not appreciably affect fog persistence (private communication with Bernard Silverman, Air Force Cambridge Research Lab).

In previous laboratory investigations (Jiusto, 1964) we have shown that while ionic surfactants can reduce a water droplet's surface tension by as much as 60% and alter the surface ion distribution, no significant difference in the diffusional growth (or evaporation) rates of treated and untreated droplets exists. Non-ionic, long chain alcohols such as octadecanol and hexadecanol, however, were shown to drastically retard water vapor penetration and hence reduce both the rate of evaporation and diffusional growth rate of treated droplets. During the past year we have extended our investigation of surface active materials to determine whether or not the coalescence rates of droplets could be altered by treating them with surfactants.

To test the hypothesis that droplets treated with ionic surfactants coalesce more easily than do untreated droplets, we set up experiments in which the collision of individual drops with a plane water surface was observed. A vibrating capillary device was constructed with which stable streams of uniformly sized droplets could be produced; Mason, Jayaratne, Woods (1964). The instrument consists of a hypodermic needle attached to the center of a diaphragm of an earphone. An audio frequency oscillator is used to drive the earphone and cause the needle to vibrate. By forcing water through the hypodermic needle at a constant rate and by adjusting the oscillator to drive the needle in one of its resonant modes, stable streams of droplets from 50 to 500μ radius can be produced. To observe the droplets issuing from the needle tip, a stroboscopic lamp adjusted to the oscillator frequency, is used to illuminate the droplets, thereby creating the illusion of a stationary stream of droplets. Frequently several streams of droplets are flung from the needle

in various directions, but by careful adjustment of the rate of flow through the needle and the frequency and amplitude of oscillation, a single stream of droplets can be produced. By adjusting the angle of incidence of the impinging droplets on the plane water surface and the flow rate of the droplet stream, droplets can be made either to coalesce immediately or to bounce, and even skid, along the water surface for several centimeters before coalescing.

In order to investigate the effects, if any, of surfactants on droplet coalescence, the apparatus was arranged to cause a single stable stream of untreated 300μ radius drops to strike the water surface. The droplet stream was adjusted so that all drops colliding with the water surface would coalesce immediately. Then, without disturbing the apparatus in any other way, a small amount of ionic surfactant was added to the plane water surface. Almost instantly, droplet coalescence was greatly retarded and impinging drops began to bounce several centimeters in the air! After one or two bounces the drops would skid along the treated surface, not coalescing until their forward motion had nearly stopped. After bouncing, many drops would often coalesce with one another producing still larger drops before coalescence with the plane water surface.

These results are illustrated in Figures 13 through 17. In each set of photographs droplet coalescence is compared before and after the addition of a small amount of surfactant to the water surface. Generally, 1 part of a 10% solution of surfactant in 10,000 parts water is sufficient to inhibit coalescence substantially. In figures 13, 14, and 15, the effect of treating water surfaces with anionic, cationic, and non-ionic surfactants, respectively, is shown. The surfactants used were sodium tetradecyl sulfate, 1 hydroxy-ethyl-2 heptadecentyl glyoxalidene, and a type of nonyl phenyl polyethylene glycol ether. Experiments with other types of ionic surfactants yielded experimentally similar results. Crystals of hexadecanol (a fatty-alcohol, insoluable in water) were also tested. Again, droplet coalescence was inhibited as illustrated in Figure 16, although the response of droplets to the addition of this monolayer was substantially slower, presumably because

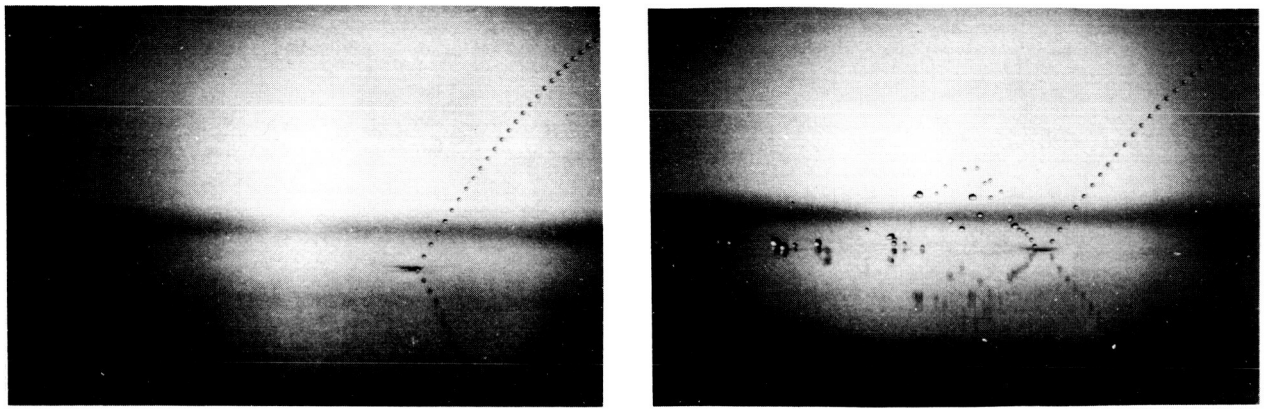

(a) Before (b) After

Figure 13 300 μ RADIUS WATER DROPS IMPACTING AT 95 cm/sec ON A PLANE WATER SURFACE BEFORE AND AFTER TREATING THE WATER SURFACE WITH ANIONIC SURFACTANT (sodium tetradecyl sulfate)

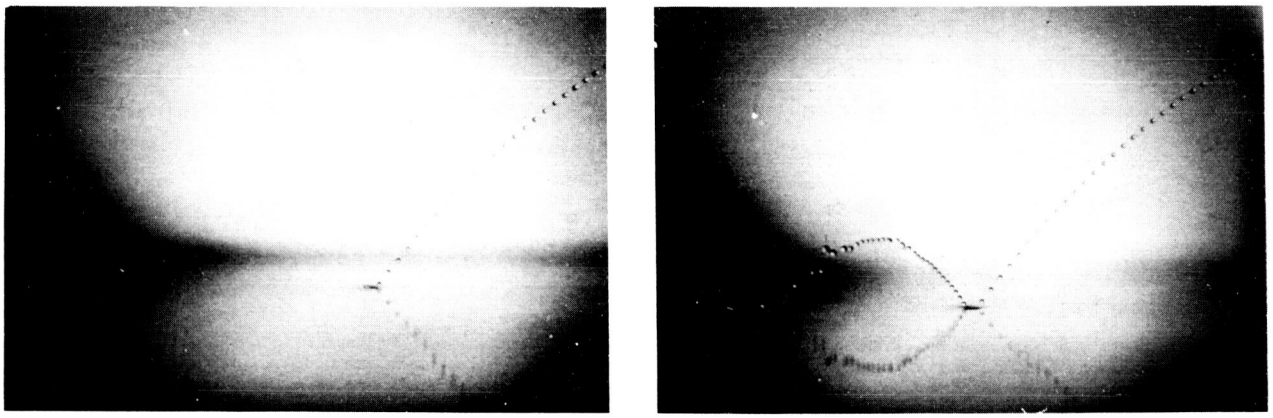

(a) Before (b) After

Figure 14 300 μ RADIUS WATER DROPS IMPACTING AT 105 cm/sec ON A PLANE WATER SURFACE BEFORE AND AFTER TREATING THE WATER SURFACE WITH CATIONIC SURFACTANT (1 hydroxyethyl, 2 heptadecentyl glyoxalidene)

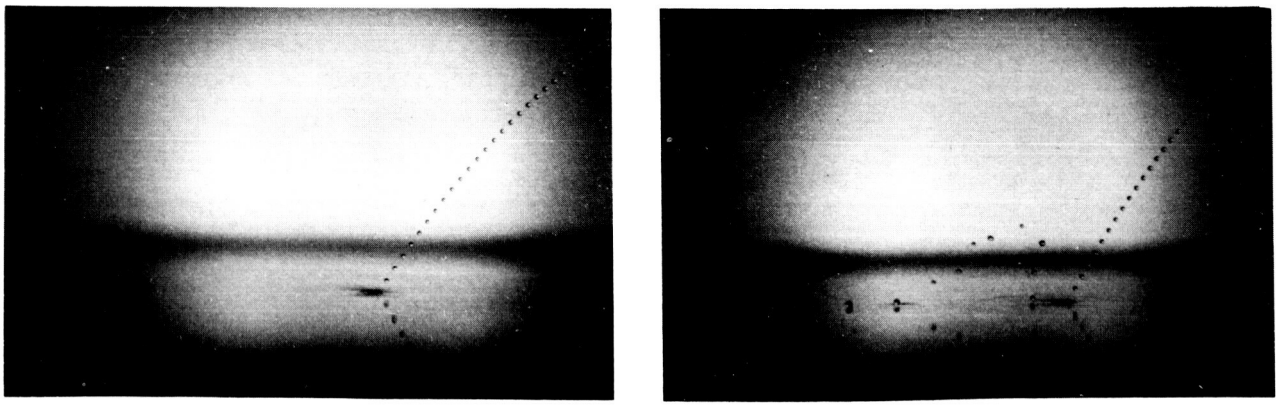

(a) Before (b) After

Figure 15 300 μ RADIUS WATER DROPS IMPACTING AT 100 cm/sec ON A PLANE WATER SURFACE BEFORE AND AFTER TREATING THE WATER SURFACE WITH NON-IONIC SURFACTANT (a type of nonyl phenyl polyethylene glycol ether)

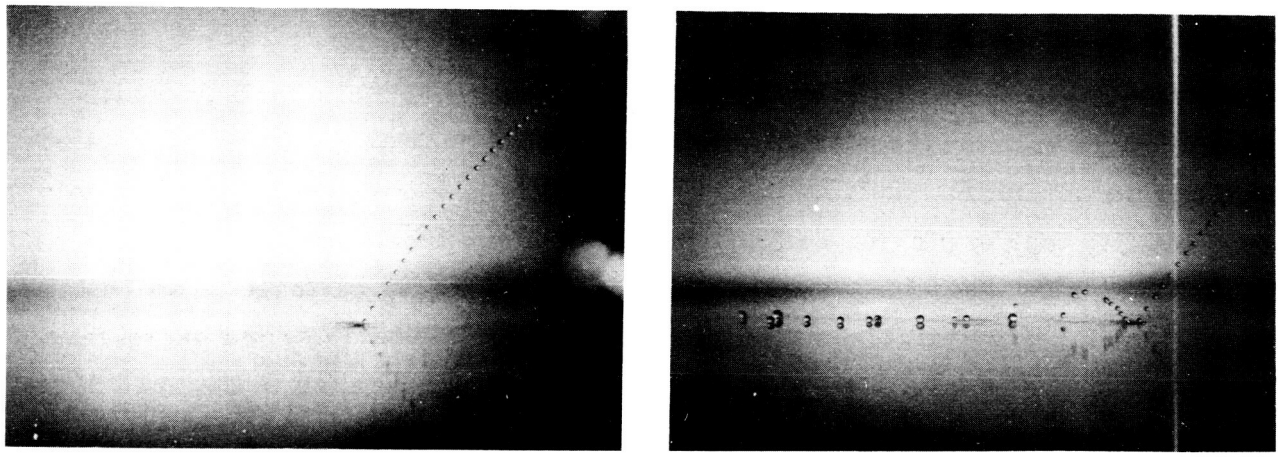

(a) Before (b) After

Figure 16 300 μ RADIUS WATER DROPS IMPACTING AT 100 cm/sec BEFORE AND AFTER TREATING THE WATER SURFACE WITH HEXADECANOL CRYSTALS

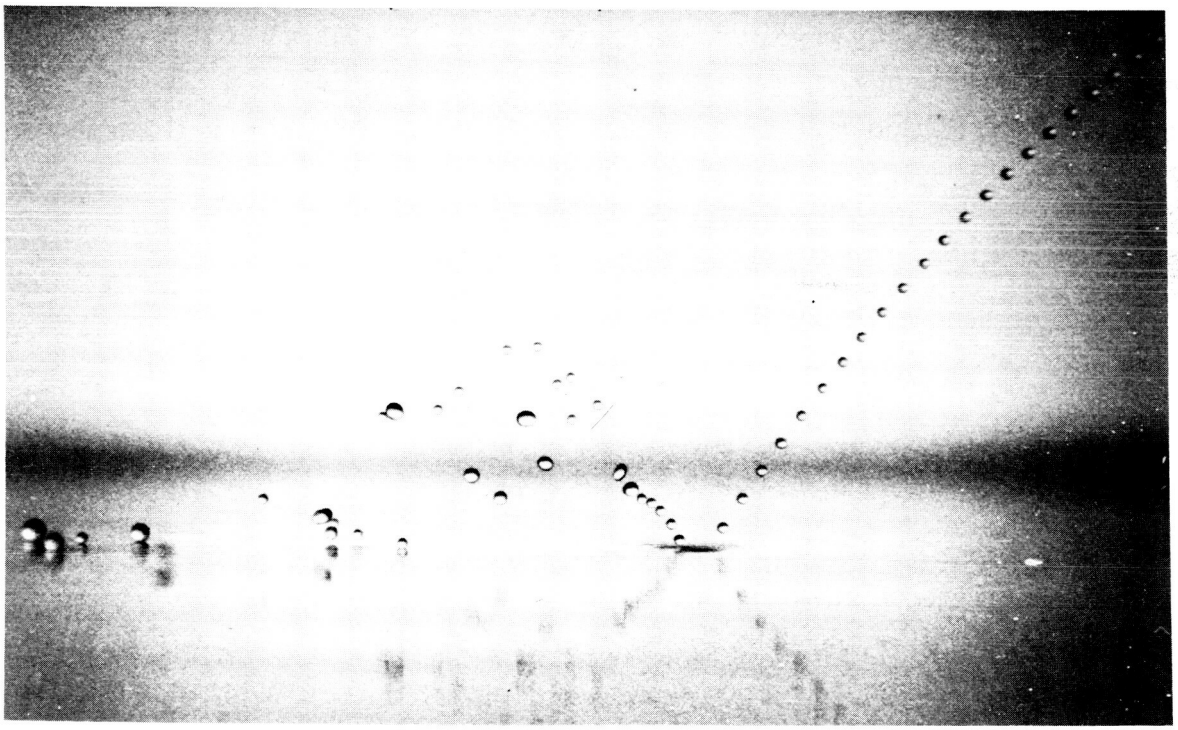

Figure 17 ENLARGED PHOTOGRAPH OF Figure 13b SHOWING DROPS IMPACTING AND BOUNCING ON A TREATED WATER SURFACE. AT IMPACT, DROPS FORM A CRATER ABOUT THREE DROP DIAMETERS WIDE

of the slower spreading rate of hexadecanol crystals.

In the photographs presented, the water drops are of approximately 300μ radius and are impacting with the plane surface at about 100 cm/sec. To emphasize the inhibition of drop coalescence and to point out the substantial impact velocity that impinging droplets have, note that drops striking the treated water surfaces form a crater which at times is two or three drop diameters wide. This effect is particularly apparent in the enlarged photograph shown in Figure 17. The skidding of drops is exemplified in Figures 13b and 16b. It is clear from these photographs that many drops, after bouncing once, have coalesced with one another to form larger drops. From the ratio of initial to final drop diameters, it appears that in some cases as many as eight to ten drops coalesce to form a single large drop resting on the plane water surface. The large drops, were found not to coalesce with the treated water surface until they were nearly stationary.

We were aware that drops issuing from the needle tip probably carried a net charge that could influence our results. To measure the charge on individual water drops we used the charge concentration meter developed at CAL. Briefly, the unit consists of a cylindrical Faraday cage having an electrostatic field meter mounted in its wall. Sample drops were allowed to pass through the cylinder and the electric field due to the droplet charge within the chamber was sensed and recorded. Normal charge on individual 300μ radius drops was determined to be 2.8×10^{4} electronic charges or 5.7×10^{-16} coulombs. Drops could be neutralized (to within the minimum meter sensitivity of $\pm 3 \times 10^{3}$ electronic charges) by applying a voltage of proper polarity between the needle and a copper shield surrounding the needle tip and part of the drop stream. We found, however, that in all of our experiments, drop coalescence (or bouncing) was not affected noticeably by the charge ($\pm 10^{-16}$ coulombs/drop) normally present on individual drops. We therefore decided it would be unnecessary to neutralize drops prior to observing drop coalescence.

Tests were also performed to determine whether drops striking the treated water surfaces were actually bouncing or causing the bulk water to splash at impact. Ink was introduced into the bulk water to serve as a color tracer and the surface was treated with surfactants. The impinging drops were permitted to bounce once and then were collected in glass vials. The collected water was compared with an equal amount of the water containing the tracer. None of the dye was apparent in any of the collected samples. It was concluded, therefore, that in spite of the deep craters mentioned previously the water drops were bouncing after making momentary contact with the treated surface and that splashing was not significant if present at all.

From the results reported here we can state that in our laboratory experiments all of the surfactants studied clearly inhibited the coalescence of drops with a flat water surface. A partial explanation of these findings may be that the hydrophobic component of the surfactant molecule presents enough of a barrier to water penetration to seriously hinder drop coalescence. It is also possible that the presence of the surfactant in some way retards dissipation of the air film between surfaces, that always exists for a short time after impact, so that drops striking the treated water surface do not initially penetrate and coalesce.

It is tempting to extrapolate the results of the experiments described above, in which drops impinged on a plane water surface, to the consideration of collision and coalescence of two spherical drops. In view of the known importance of surface curvature effects on drop coalescence, such an extrapolation is dangerous. In an attempt to observe the coalescence of droplets colliding in air we have constructed a second vibrating capillary device so that two stable streams of droplets can be made to interact. The streams can be adjusted so that coalescence occurs when untreated droplets emerging from both capillaries collide. Surfactant is then added to one water reservoir without altering other experimental conditions so that we can try to determine whether or not coalescence is again inhibited. We have noted in many instances that after the surfactant has been added to the water

reservoir, the droplet stream issuing from the needle tip breaks apart in a random fashion, producing unorganized patterns of drops. This effect is apparently due to the decrease in surface tension (approximately 60%) affected by the addition of surfactant to the water. We have been able to partially overcome this problem and to produce more stable streams of droplets by using the same very dilute solutions of surfactant (1:10,000) used with the plane water surface. To date, we have not been able to notice any appreciable difference in the coalescence rates of treated 300μ radius drops colliding in air. The effect of treatment, however, may have been partially obscured by the very high coalescence efficiency characteristic of such large drops. Before definite conclusions can be drawn it will be necessary to experiment with colliding droplets having sizes more nearly characteristic of natural fog (i.e. $\sim$ 50μ diameter).

2. Condensation nuclei deactivation

We have hypothesized that if a percentage of the condensation nuclei active in natural fog can be deactivated prior to fog formation, the resultant fog might consist of fewer, larger particles that 1) fall out faster and 2) scatter less light per unit mass of water and thereby reduce the visibility restriction. Preliminary experiments conducted during the first year of this project showed that it was possible to reduce the growth rate of drops formed on treated hygroscopic nuclei, but the result of efforts to prevent hygroscopic nuclei from hydrolizing were inconclusive. Further experimentation was recommended.

More recently we have conducted experiments to determine whether sodium chloride crystals, known to be active at relative humidities of 72-75%, can be prevented from participating in droplet growth when treated with fatty-alcohol monolayers. A simple set of apparatus described by Jiusto and Pilié (1958) was used to produce controlled conditions of humidities up to 98%. Grains of sodium chloride were pulverized and placed on a clean glass slide where they were examined under a microscope while being exposed to the controlled atmosphere. On another slide, similar NaCl

crystals were coated with a solution of hexadecanol dissolved in petroleum ether. Petroleum ether quickly evaporates so that a residual coating of hexadecanol remains on those nuclei coming in contact with the solution.

Initial observations indicated that coated NaCl crystals could be prevented from hydrolizing at relative humidities up to 90%. We felt, however, that the surfactant layers produced in these experiments were too thick for a realistic evaluation and therefore experimented with methods of producing very thin layers of hexadecanol on the crystals. The desired method of coating was accomplished by using about 0.1 g hexadecanol or octadecanol in 10 g of petroleum ether and applying the solution to the crystals. Salt crystals treated in this manner were uniformly coated with surfactant.

To determine the effectiveness of treating nuclei we first examined untreated crystals and observed their nucleating behavior at various relative humidities. In Figures 18a and 18b photographs are presented showing untreated NaCl crystals before and after exposure to air at 76% R.H. Note

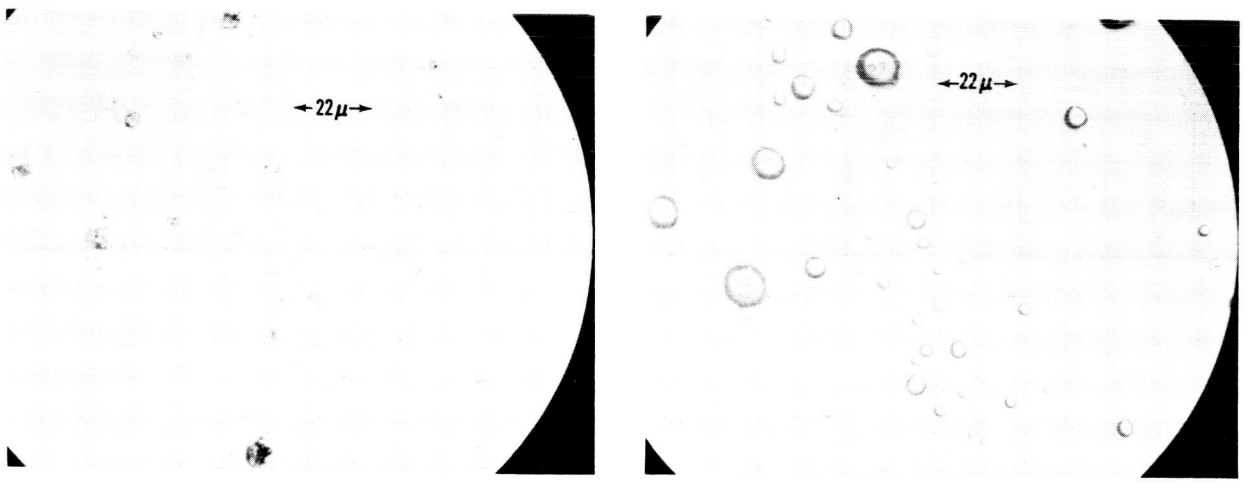

(a) Before (b) After

Figure 18 UNTREATED NaCl NUCLEI BEFORE AND AFTER BEING EXPOSED TO AIR AT 76% RELATIVE HUMIDITY FOR THREE SECONDS

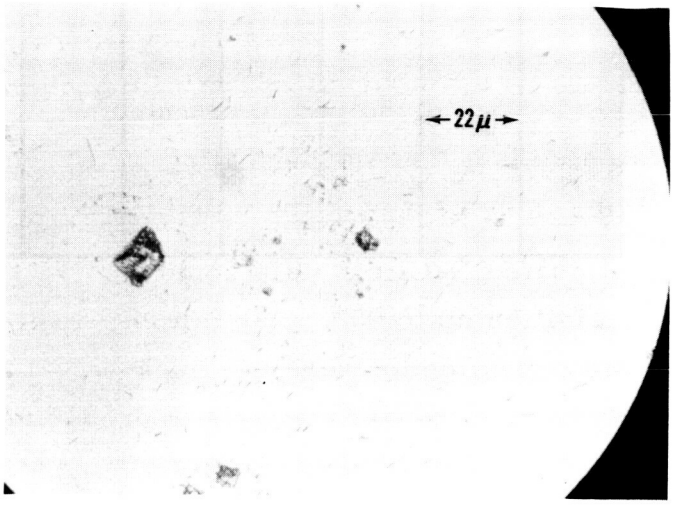

(a) NaCl nuclei treated with a layer of hexadecanol

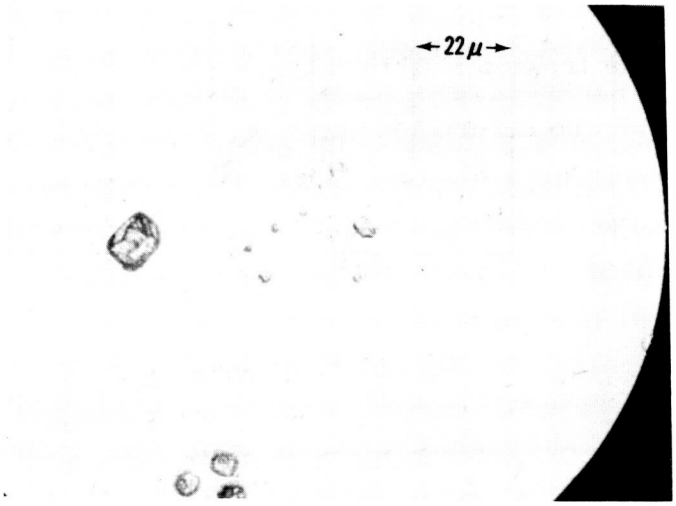

(b) Same nuclei after exposure to 75% R.H. for 15 seconds

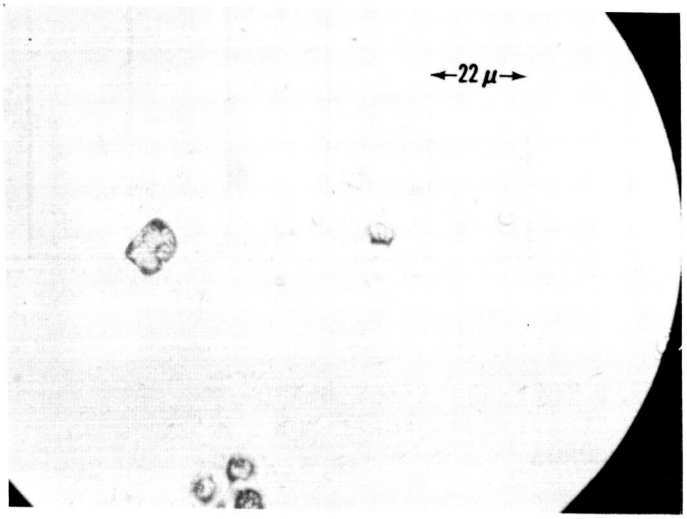

(c) Same nuclei after exposure to 80% R.H. for 15 seconds

Figure 19

that in Figure 18b each of the salt nuclei has served as a condensation site and has produced a small droplet after a comparitively short period of 3 seconds. In sharp contrast with these results the photographs of salt nuclei treated with a thin layer of hexadecanol (Figures 19a-19c) indicate substantial retardation of droplet growth. The fibrous, hair-like structures in the photographs are crystals of hexadecanol that have remained after the petroleum ether evaporated. In Figures 19b and 19c the treated nuclei are shown undergoing various stages of droplet growth after 15 seconds exposure to 75% and 80% R.H. respectively. It is clear from these photographs that the crystals treated with hexadecanol have only started to hydrolize after 15 seconds whereas untreated crystals form small drops at comparable relative humidities in only 1/5 the time.

We may conclude that while treated nuclei are not deactivated when exposed to relative humidities greater than 75% their subsequent rate of growth is substantially retarded. These results, while encouraging, are not sufficient to warrant large scale treatment of atmospheric nuclei. Clearly, even if condensation nuclei could be appropriately coated in the atmosphere, their participation as nucleating sites for natural fog droplets would not be prevented, but would only be retarded. This does not rule out the potential application of these results where suppression of fog formation is desired while still another means of treatment is attempted. There remains, however, the sizeable task of devising effective means of treating large populations of nuclei in the atmosphere. When and if such a method is devised, these results could provide a starting point for future investigations directed toward fog modification.

C. Condensation Nuclei Measurements*

1. Thermal diffusion chamber

The concentration, size and hygroscopic activity of condensation nuclei in the atmosphere largely determines the supersaturation achieved in fog and the resultant drop size distribution. Chemical and thermal diffusion chambers, which are described in the First Annual Summary Report, are well suited for measuring the concentration of nuclei active at slight supersaturations typical of fog. A more complete description of the portable thermal diffusion chamber and the operating procedure we are using for making nuclei measurements is given below.

The chamber is constructed of lucite tubing having a sampling volume 9.9 cm in diameter and 1.7 cm high. A second larger cylinder of lucite surrounds the inner chamber and provides additional protection against heat transfer through the walls. A circular lucite plate separates the two chambers and contains the insulating air jacket between them. To maintain precision control of the lower water surface and to allow a wide range of operating temperatures a constant temperature circulator is being used. Cotton balls that have been saturated with water provide an upper water reservoir which is maintained at essentially ambient wet-bulb temperature.

The optical system for recording droplet concentrations within the diffusion chamber consists of an intense light source and associated optics to illuminate a known volume of the fog and a polaroid camera to record light that is scattered by droplets in the cloud chamber.

A mercury arc lamp (Osram No. HBO 100 W/2) is used as the light source. The lamp arc is focused onto two fixed slits by a pair of large condenser lenses. The slits are 0.15 x 0.5 cm in cross section. Another set of lenses is used to form the slit images within the diffusion chamber resulting in a well defined light beam that has cross section dimensions equivalent to those of the defining slits. To reduce light losses and eliminate image distortion by the curved lucite walls, the chambers have been fitted with plane glass windows.

*By Warren C. Kocmond

A polaroid camera (Dumont Type 302) is located with its axis at right angles to the light beam. The light that is scattered by a droplet within the cloud chamber is focused onto the polaroid film and recorded. A frosted glass can be used in place of the film for preliminary setup procedures and for visual observations of droplet concentrations within the chamber. The camera has a 1 to 1 magnification and, in conjunction with the fixed illuminated volume, is used to photograph the droplets in a sample volume 0.15 x 0.5 x 1.0 cm. The system is completely portable; four heavy duty wet cell batteries supply ample power for 8 continuous hours of operation.

To facilitate outdoor nuclei measurements and to minimize temperature fluctuations during operations, the portable chamber and its associated equipment is housed in insulated cabinets. A 28 volt d.c. to 110 volt 60 cycle a.c. converter, having a power output of 750 watts, allows battery operation of the electrical components.

In order to study actual droplet sizes within the chamber we prepared glass slides with a thin layer of oil and captured cloud droplets at relatively high supersaturations (about 10%). The treated slides were placed under a prefocused microscope and photographed within 10-15 seconds of droplet capture. Because micron size droplets, even when immersed in a layer of oil, will evaporate fairly rapidly when exposed to dry air, the slides were photographed as quickly as possible after obtaining a specimen. Droplet diameters were found to be in the range 2 to 10 microns, as shown in Figure 20. These values are consistent with observations of the fall velocity of droplets in the chamber.

In preliminary attempts to photograph fog droplets various experimental chambers were used, all with height-to-diameter ratios of approximately 1/2. We found that, while photographs could be made at supersaturations of 5% and larger, considerable difficulty was encountered in obtaining data below 1% supersaturation. It was determined that under low supersaturations the excess water vapor in the vicinity of the droplets was reduced by condensation at a rate faster than it could be replaced by diffusion from the upper reservoir. Hence the ambient supersaturation

Figure 20 FOG DROPLETS CAPTURED IN THERMAL DIFFUSION CHAMBER

was actually substantially lower than that computed from measured temperatures. This difficulty was resolved by decreasing the distance between the water surfaces to a height to diameter ratio of 1/6 so that the vapor flux was greatly increased and enough water vapor was available through molecular diffusion to maintain the calculated supersaturations.

Exhaustive temperature measurements were made within the sampling volume of the chamber. These tests indicated that when the water surfaces are close together, e.g., a height-to-diameter ratio of 1/6, a linear vertical temperature profile can be assumed so that measurements of temperature need only be made at the two surfaces of the water reservoir, rather than at intermediate heights throughout the sampling volume as originally thought necessary.

We found with this configuration that accurate and reproducible measurements can be made at supersaturations as low as 0.02%. Accuracies of approximately ±0.1% supersaturation can be achieved on a routine basis for desired supersaturations larger than 1.0%. For smaller desired values the accuracy is improved to approximately ±0.01% supersaturation.

2. Measurement of atmospheric nuclei

During the winter months measurements of atmospheric nuclei were made from inside the Cloud Physics Laboratory. To facilitate indoor measurements the laboratory has been equipped with an air intake duct constructed of 2" copper tubing. A fan continually draws outside air through the duct and past a sampling tap, which allows the air to be aspirated into the chamber by a small vacuum pump having an adjustable rate of flow. A three way solenoid valve is positioned ahead of the chamber inlet to allow the sampling volume of the chamber to be flushed with nitrogen prior to admitting atmospheric nuclei.

Recently the thermal diffusion chamber has been transferred to a mobile van to facilitate nuclei measurements in different locations. Initially, these measurements were made on the premises of CAL and later a nuclei survey was conducted near Springville, N. Y., (a rural area which is comparatively free of atmospheric pollution).

The observational technique and sampling procedure used is as follows: the upper and lower water reservoir temperatures are carefully adjusted to permit the system to come to equilibrium at a predetermined supersaturation. When the desired temperature differential has been achieved, nuclei to be investigated are aspirated through the chamber at a continuous rate for 5 to 6 seconds. (It is important to avoid pressure changes within the chamber during the sampling period; e.g., clearly, spuriously high supersaturations will prevail if a partial vacuum is created within the chamber.) Once inside the chamber, the air sample is allowed to reside in the supersaturated environment, where in a few seconds, those nuclei that are activated under the existing supersaturation grow to droplet size and become visible in the intense light. The droplets continue to grow until they are several microns in diameter, and then settle out. Other nuclei that are not active, simply remain suspended in the air sample but do not participate as obserable droplets in the ensuing cloud. Photographs of fog drops are taken a moment before sedimentation begins which can be easily estimated after a little experience. Sample photographs are shown in Figure 21. The photographs shown have been enlarged for presentation here.

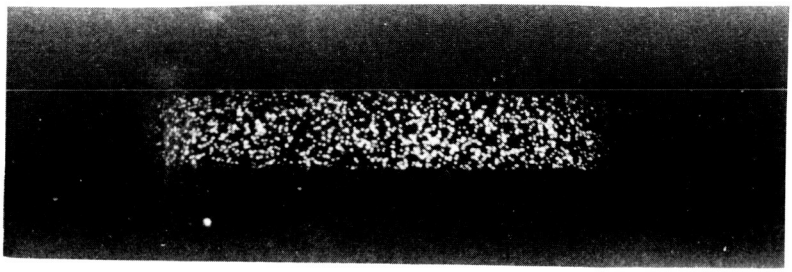

(a) Water droplets formed at 3.0% supersaturation 5000 drops/cm^3

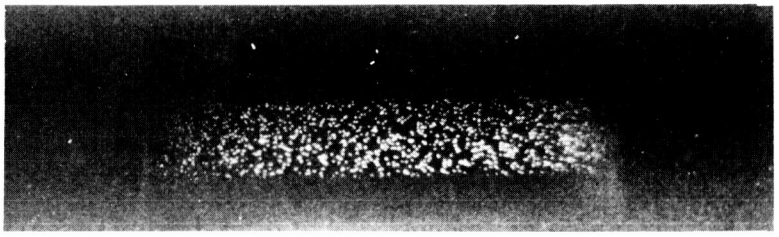

(b) Water droplets formed at 0.9% supersaturation 4200 drops/cm^3

(c) Water droplets formed at 0.3% supersaturation 1050 drops/cm^3

(d) Water droplets formed at 0.1% supersaturation 500 droplets/cm^3

Figure 21 PHOTOGRAPHS OF FOG DROPLETS FORMED AT VARIOUS SUPERSATURATIONS IN THERMAL DIFFUSION CHAMBER

Generally, three or four samples are photographed for each supersaturation. The number of active nuclei is estimated from droplet counts made through an overlay which defines a sensitive portion of the photograph measuring 0.42 x 0.92 cm corresponding to a sensitive volume in the chamber of 0.072 cm^3.

We have assembled data from daily measurements for about a 1/2 year period at the CAL site and for a one week period near Springville. From these data several fundamental features of atmospheric nuclei concentrations have been observed which, when analyzed in conjunction with other meteorological data, allow us to draw certain conclusions about the variation and concentration of nuclei active at slight supersaturations.

In Table I results of observations in the Buffalo and Springville, N. Y. area are presented which represent average nuclei concentrations in these areas as a function of supersaturation.

Table I

Average Nuclei Concentrations in Buffalo and Springville Areas

Supersaturation	Average No. of Nuclei/cc^3 (Buffalo, NY area)	Average No. of Nuclei/cc^3 (Springville, NY area)	% Difference at 2 sites
3.0%	5300	3075	42%
0.9%	3450	1725	50%
0.1%	495	415	19%
0.02%	425	335	21%

It is immediately apparent from these figures that the concentration of nuclei in the Springville area, particularly at 3.0% and 0.9% supersaturation, is substantially smaller than observed at CAL. The more pronounced effect at higher supersaturations can be explained in the following manner:

In a polluted atmosphere much of the aerosol is comprised of Aitken nuclei (particulates in the 10^{-5} to 10^{-6} cm size range that are primarily combustion products). Generally, these very small particles are neither large enough nor hygroscopic enough to initiate droplet growth at very low supersaturations. When exposed to a slightly supersaturated environment they become enlarged haze particles but usually do not participate as observable droplets. If the supersaturation is increased, smaller Aitken nuclei can serve as condensation sites for fog droplets, however, in order to activate the smallest and least hygroscopic of these nuclei supersaturations of over one hundred percent are sometimes required (certainly an unattainable supersaturation in the free atmosphere). For this reason most of the industrial contaminants do not appreciably influence nuclei counts at very low supersaturations, as the data in Table I indicate. On the other hand, at slightly higher supersaturations (i.e. 0.9% and 3.0%), enough excess water vapor is available to permit condensation on some of the larger Aitken nuclei; hence evidence of atmospheric pollution becomes increasingly obvious.

It should be noted that the effects of pollution are never completely hidden even at extremely low supersaturations. Since nuclei are constantly in motion, many of the smaller Aitken particulates agglomerate with one another to form larger, and hence, more favorable condensation sites. That this is constantly taking place is shown by the somewhat higher numbers of "fog nuclei" in the Buffalo (relative to Springville) area even at 0.02% supersaturation. It should be emphasized however that the effect of atmospheric contamination is more than twice as great at the higher supersaturations.

In previous reports we have suggested that representative droplet concentrations in natural radiation and advection fogs are 200 cm^{-3} and 40 cm^{-3}, respectively. It would appear from Table I, therefore, that saturation in natural fog rarely exceeds a few hundreths of one percent.

The concentrations of nuclei active at various low supersaturations during periods of precipitation have been reasonably well established for the CAL site. These results are compared in Table II with data obtained during non-precipitation conditions. Precipitation cases include instances of general rain or snow as well as cases in which only flurries (showers) or squalls were reported. These numbers verify the well known effect of nuclei removal associated with precipitation. The effect is more pronounced than is shown in Table II during episodes of widespread precipitation, but too few of these cases have been observed for statistical evaluation. It appears from these data that scavenging is most effective for the nuclei that are active at extremely low supersaturation.

Table II

Effect of Precipitation on
Average Nuclei Concentration

Supersaturation	Average Nuclei/cm^3 No Precipitation	Average Nuclei/cm^3 Precipitation	% Nuclei Reduction (Scavenging)
3.0%	5670	4570	20%
0.9%	3740	2890	23%
0.3%	1090	845	24%
0.1%	570	350	39%

Two cases were observed in which the decrease in nuclei concentrations associated with precipitation was particularly apparent. The data for these cases is shown in Table III. The average values for all Buffalo observations are included for comparison.

Table III

Two Examples of Nuclei Reduction
Associated With Precipitation

Supersaturation	Nuclei/cm^3 (Jan. 27, 1965)	Nuclei/cm^3 (Feb. 7, 1965)	Average No. of Nuclei/cm^3 All Cases
3.0%	7100	1400	5300
0.9%	4100	1250	3450
0.3%	350	500	1000
0.1%	280	270	495

In the first case, Jan. 27, 1965, the observations at 3.0% and 0.9% had been completed when a heavy snowsquall developed. Measurements at 0.3% and 0.1% supersaturation were made during the squall. Prior to the snowsquall, counts were substantially above average as the figures for 3.0% and 0.9% indicate. With the onset of heavy snow, the numbers of active nuclei fell far below average. For instance, the concentration of nuclei active at 0.3% supersaturation was 65% below the mean value for all dates. A similar but not as drastic change was noted at 0.1% supersaturation.

The fact that the very low concentrations were observed shortly after onset of precipitation may be interpreted in two ways: The scavenging process could have been extremely efficient causing very rapid removal of nuclei. On the other hand the onset of precipitation could have been accompanied by a sudden downdraft of cleaner air from aloft similar to that often associated with thunderstorms. It does not seem unreasonable that both effects took place simultaneously.

The second case occurred on Sunday, February 7, 1965 when urban pollution was minimized because of lessened industrial activity and a favorable ESE wind (Cornell Aeronautical Laboratory is located about 10 miles east of downtown Buffalo). Widespread precipitation had been falling for several hours prior to making nuclei measurements. As indicated in Table III, the concentration of nuclei was substantially below average at all supersaturations tested. In this case the normally low concentrations of active

nuclei accompanying southeast winds appeared to be decreased even further by the scavenging effect of widespread precipitation. These data indicate further, that even after widespread precipitation several hundred drops/cm^3 can be formed at 0.1% supersaturation. These measurements, of course, only apply to a continental region such as Buffalo. In an effort to learn more about the concentration of nuclei that are active at low supersaturations in a maritime climate, observations are currently being made on the island of Hawaii under the auspices of another CAL program.

A statistical evaluation was performed to determine the variation of nuclei as a function of wind direction. The statistics obtained are indicative of the effects of pollution described earlier in this section. As expected, urban pollution was found to be a major contributor to the number of nuclei active at supersaturations in excess of 1.0%. On the other hand, we found that a fairly poor correlation existed between urban pollution and active nuclei near 0.1% supersaturation. These observations are illustrated in Figures 22 and 23. The extremely high counts at all supersaturations during periods of northeast wind are due to factory smoke emitted within a quarter mile of our air sampling duct.

The results of our measurements to date permit us to draw two conclusions that have particularly important implications for cloud (fog) physics. One, is that local sources of atmospheric pollution are by no means the most important contributors to fog nuclei, i.e., nuclei active at very low supersaturations. Pollution will, of course, seriously restrict visibility when the humidity is high since such particulates become slightly enlarged and contribute to industrial haze. The presence of contaminants, however, does not necessarily mean high concentrations of fog nuclei, since polluted air is at times characterized by lower than average concentrations.

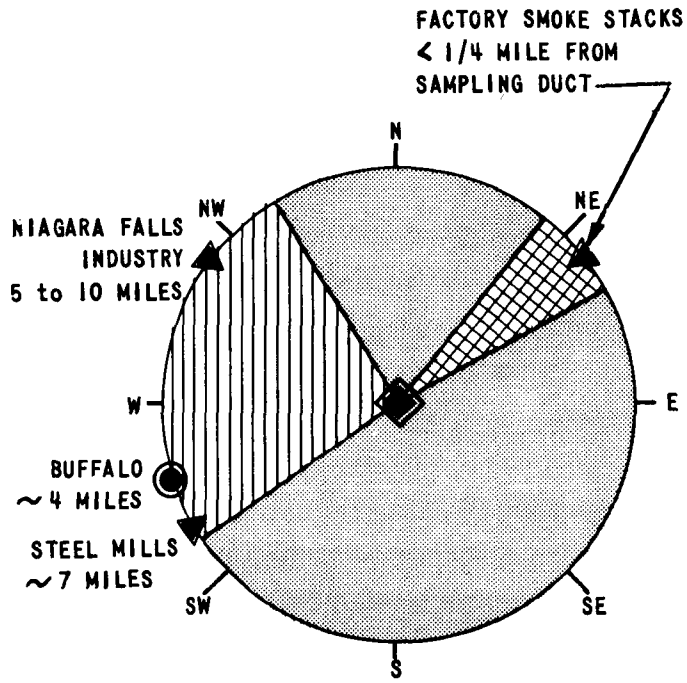

Figure 22

VARIATION OF NUCLEI CONCENTRATION AT 3.0% SUPERSATURATION AS A FUNCTION OF WIND DIRECTION

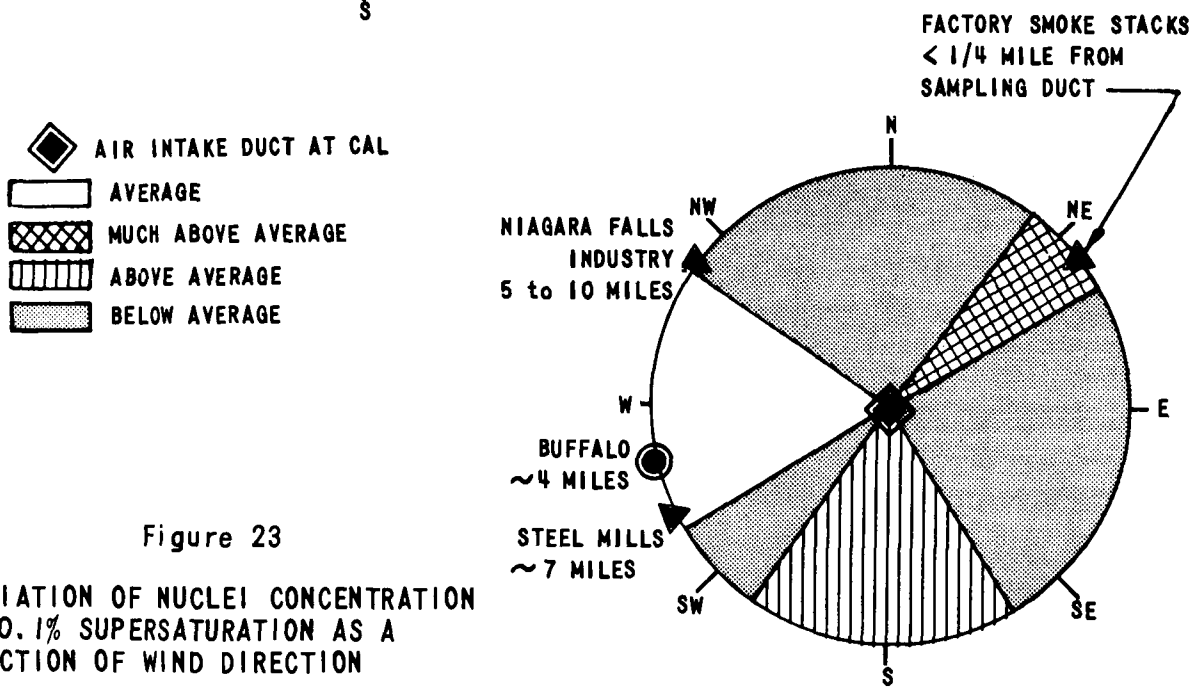

Figure 23

VARIATION OF NUCLEI CONCENTRATION AT 0.1% SUPERSATURATION AS A FUNCTION OF WIND DIRECTION

The second, and perhaps more important, conclusion is that in continental regions, at least, the concentration of nuclei that can be activated to droplet growth even at 0.02% supersaturation exceeds the concentration of droplets found in fog. This implies that in natural fog, supersaturations greater than a few hundreths of a percent are seldom achieved except in transient situations.

These results point out the need for continued measurements of nuclei concentrations at extremely low supersaturation to help define the number and type of nuclei that are responsible for natural fog. It may even be necessary to observe those nuclei that serve as nucleating sites at 100% relative humidity. Furthermore, in a recent review of our data we have noted what appears to be a correlation between nuclei concentrations and ambient relative humidity, such that the concentration of fog nuclei in the free atmosphere is usually high when the relative humidity is high. We have hypothesized that as the humidity increases nuclei that were formerly inactive become potential sites for condensation at slight supersaturations. This, of course, suggests that some nuclei become active only after prolonged exposure to fairly high relative humidity. If this hypothesis is correct, fog density may, in part, be determined by the history of nuclei exposure to relative humidity. An attempt to examine this hypothesis is planned.

D. Drop Size Measurements in Natural Fog*

Slides treated with a 5% solution of gelatin are being used to obtain permanent replicas of the drop size distribution in natural advective and radiation fogs occurring in the Buffalo area. Such experiments will contribute to the meager information now available on drop sizes in fog. To date, four advection and three frontal-type fogs have been observed and droplet replicas made. The drop diameters in these fogs were found (as expected after long exposure to a supersaturated environment) to be several microns larger than droplets formed in the thermal diffusion chamber. The average minimum and maximum drop sizes observed during the four advection fogs was 6μ and 63μ respectively, and for the three frontal fogs 4μ and 52μ respectively. High and low values of 95μ and 1μ were observed in these fog types but more than half of all drops were less than 21μ in diameter. While these results are in good agreement with the data given by our physical fog models, (see First Annual Summary Report), it is probable that future measurements will indicate lower average drop diameters, since our method of sampling has been improved recently by using very narrow slides (5 mm wide) to minimize preferential capture of large drops. To date no radiation fogs have been observed, however, during the fall months we expect to conduct a field trip to a region having fairly frequent, dense radiation fog to obtain more information about certain fog parameters and to verify and improve our physical and dynamic radiation fog models. Measurements will be made of average drop diameter, drop size range, nuclei concentration, horizontal visibility, and vertical depth of fog. Representative measurements of these pertinent fog values will provide the type of information that is essential for successful fog modification.

---

*By Warren C. Kocmond

E. Formulation of Fog Alteration Concepts*

1. Program findings

Three concepts for fog suppression have been advanced on this project. These concepts are based on the facts that a) the terminal fall velocity of a droplet is directly proportional to the square of its radius, and b) for constant liquid water content the amount of light scattered by an ensemble of fog particles is inversely proportional to droplet radius. The new concepts are therefore aimed at redistributing fog liquid water from a large number of small droplets to fewer larger droplets that would a) precipitate faster and b) scatter less light. These concepts are:

a. Minimize the competition for available water by treating a portion of the droplet population with certain monolayers to retard growth of the treated aerosol and permit more rapid growth of the untreated droplets. This concept was discussed in the first annual report.

b. Promote droplet coalescence by electrically charging droplets positively and negatively in alternate adjacent regions of a fog. Such a treatment will 1) establish a mutual attraction between droplet populations in adjacent regions to promote relative motion of droplets and increase the probability of collisions 2) after mixing of the drops from adjacent regions has been established, promote coalescence of oppositely charged drops by coulomb attraction between individual drops. The desired redistribution of liquid water in the form of fewer, larger drops should ensue.

c. Prevent activation of most of the natural condensation nuclei that are normally active in fog by artificially introducing a relatively small number of large, extremely hygroscopic nuclei into the atmosphere prior to the formation of fog. The nature of the artificial nuclei must be such that they grow at relative humidities that are too low for activation of most natural nuclei while the number must be sufficient to suppress supersaturation. If sufficiently active nuclei can be produced the resulting fog will consist of a relatively small number of large droplets. In the suggested procedure it should only be necessary to promote early growth of a small number of drops

*By Roland J. Pilié, Warren C. Kocmond and John R. Graham, Jr.

on extremely hygroscopic nuclei so that all excess water vapor is removed at supersaturations small compared with that required for activation of most natural nuclei.

2. Fog dispersal by electrical means

Numerous investigators have shown that the collection efficiency of droplets is enhanced both by the presence of an ambient electric field and by the presence of charge on the droplets. Briefly, the earth's electric field polarizes the droplets in a uniform manner causing, for example, the bottom of all drops to be positive and the tops to be negative. When a large drop falls toward a small one, the oppositely charged portions of the two drops face each other and a force of attraction is established that is active over distances comparable to the drop diameter. This force opposes the aerodynamic forces that normally prevent collision of small drops. In a similar fashion, the presence of opposite charges on two drops leads to coulomb forces of attraction which increases the collection probability. If only one of the drops is charged, that drop sets up an electric field which polarizes uncharged drops and again the collection efficiency is increased.

The polarization forces fall off as $1/r^5$ while the forces between oppositely charged drops fall off as $1/r^2$. Thus, the latter, or Coulomb forces, would be more efficacious in the enhancement of the collection efficiency. Calculations of the probability of coalescence of drops due to the polarization forces have been made by Sartor (1960), Cochet (1951), Pauthenier (1947), and Shulepov and Dukhin (1962). Cochet, for example, says "....the utilization of drops of 30μ initial diameter, each carrying a charge of 4×10^{-4} esu, gives essentially the same results (same coalescence; translation) as uncharged drops of 120μ initial diameter with the advantage of representing a mass of water 64 times smaller." On the basis of such calculations it is natural to consider methods of charging fog droplets for fog dispersal purposes. The problem is that of placing the required charge on the fog droplets. Several investigators, notably Vonnegut and Moore (1958), have shown that it is possible to charge large quantities of Aitken nuclei in the atmosphere by means of corona discharge from a long wire stretched horizontally several meters

above the earth. Using 30 KV (d.c.) on a 7 km long wire 0.25 inch in diameter they were able to detect the ion cloud caused by the spray discharge as far as 8 km downwind.

We have suggested that a similar method might be used to charge alternate adjacent regions of a fog positively and negatively by applying an ac voltage of the correct frequency (depending on mean wind velocity) to such a wire. Such a procedure, we hypothesize, might establish long range forces (acting over several meters) that would cause mixing of droplets that were originally in the adjacent regions. Collision probability would thereby be enhanced both by the coulomb attraction of oppositely charged individual droplets and by the additional velocity imparted to these droplets by virtue of the net electric field due to the charge in the adjacent region.

Preliminary experiments have been performed in which an ac voltage of up to 10 KV (rms) was applied between an 0.008 inch wire and a wire screen in the form of a 2 ft diameter cylinder, with the wire along the axis of the screen cylinder. The current flow in the circuit was determined as a function of the applied ac voltage. The larger portion of the current was the capacitative component. As the voltage was increased, the current voltage curves showed a sudden change of slope at the onset of the corona current. Using the values of the experimental parameters in the equations shown by Cobine (1958), our computations indicate good agreement between the calculated and measured value for the voltage at which ac corona first appears. After correcting for the capacitative component of current, the corona current was found to be of the order of 10^{-6} ampere per centimeter of wire length.

Assuming a duty cycle of 0.1 second, the corona current is equivalent to the production of 10^{-7} coulombs in the atmosphere per centimeter of wire length. Let us assume that one-tenth of this charge attaches itself to the droplets within, say, 50 cm of the wire. Using the usual inverse first power formula for the field strength at the 50 cm boundary of this charged region, one finds that there exists an electric field of 360 volts/cm. Assuming

200 drops/cm^3, the average charge per drop will be 6×10^{-15} coulombs (or 2×10^{-5} esu). The electric force on such a drop in the above field will be about 2×10^{-5} dyne. By comparison, if these are 10μ radius water drops, the gravitational force acting on them would be about 4×10^{-6} dyne. Thus, their terminal velocity under the electric force will be about five times that under gravitational force, or 6.0 cm/sec rather than 1.2 cm/sec. Obviously, mixing of the positively and negatively charged drops from alternately charged regions would occur rapidly and the long range coulomb forces between individual droplets could be effective.

A schematic diagram of the apparatus is shown in Figure 24a. The corona current was derived from the voltage drop across resistor R_1 (corrected for the input impedance of the vacuum-tube voltmeter, VTVM). In order to determine the mobilities of the ions produced, the circuit was modified to that shown in Figure 24b. A biased plate was set up outside the screen cylinder and at various distances from the cylinder. By the use of a switched-beam oscilloscope, both the voltage drop across R_2 (due to ion collection) and that across R_3 (in phase with applied ac voltage) were displayed on the CRO. By varying the distance d between the cylinder and the collector plate, and at the same time varying the bias voltage V, the collection electric field $E (E \approx V/d)$ was kept constant. From pictures of the oscilloscope displays for two such situations, the transit times for the ions, and thus their mobilities, were calculated. The mobilities of the positive and negative ions were determined to be of the order of 1.5 to 2.0 cm^2/volt sec.

Thus far, these rather preliminary experiments have been performed using 60 cycle ac voltages. For more controlled and definitive experiments, positive or negative voltage pulses with variable pulse widths and repetition rates should be used. The mobilities measured thus far are those characteristic of fast atmospheric ions in clear air. By the use of pulsed voltages we will be able to measure not only the mobilities of these relatively fast ions but many of the less mobile ions as well. (Many ions of low mobility are formed by the attachment of fast ions to nuclei.) Further, after formation of the fast ions, a variable time delay may be used to allow the attachment

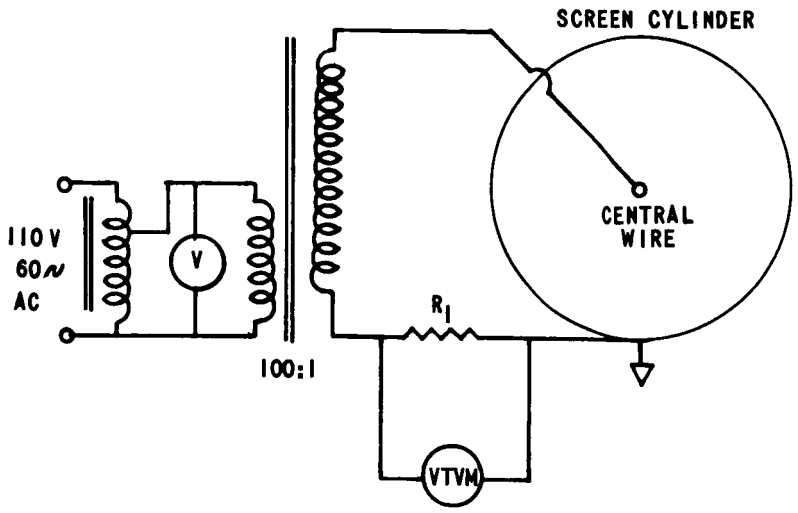

Figure 24a Schematic diagram of apparatus used to determine the voltage required to produce a corona current.

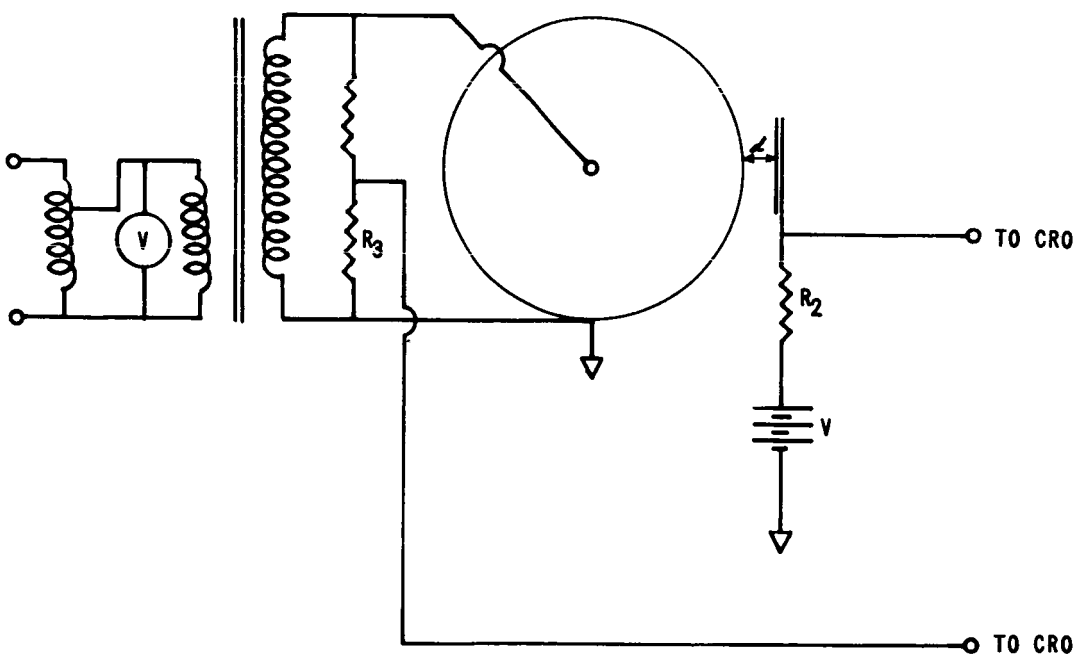

Figure 24b Schematic diagram of apparatus used to determine the mobility of ions

process to take place; the remaining fast ions may be swept out of the region and the slow ions formed may be collected and the integrated charge measured. In this way, one may determine the efficiency of the corona wire for the production of charged water droplets. Work on this phase of the experiment has already started, but actual measurements have not yet been made.

3. Possible method for preventing dense radiation fog

In the formation of natural fog, droplets undergo several related stages of growth. Initially, as the relative humidity begins to increase in an air mass, the largest and most hygroscopic nuclei absorb water vapor from the atmosphere and become enlarged haze particles. If the relative humidity continues to rise these nuclei absorb additional water vapor from the air and become solution droplets. Droplet equilibrium is established with the environment at the ambient vapor pressure and temperature. As the relative humidity approaches 100% the solution droplets continue to grow, becoming more dilute but maintaining equilibrium with ambient conditions. At the same time other nuclei of less hygroscopic material may start to hydrolize. Normally, haze begins to intensify at 70% relative humidity although the conditions of visibility depend on the number, type, and size of participating nuclei.

As soon as slight supersaturation is achieved, a limited number of solution droplets that formed on the largest and most hygroscopic nuclei begin to grow without limit. The number of nuclei that participate in the ensuing cloud is determined by a) the distribution of size and hygroscopicity of the nuclei and b) the rate at which excess water vapor is made available for droplet growth; equilibrium vapor pressure is established when the rate of extraction of water by the participating nuclei is equal to the rate at which excess water is made available. Our nuclei concentration measurements almost invariably show that the number of nuclei that are active at 0.1% supersaturation exceeds by at least a factor of two the number of drops found in natural fog. Therefore, we can conclude that the maximum supersaturation common to urban fog is small compared to 0.1%.

Furthermore, we have observed in the thermal diffusion chamber that if the availability of excess water vapor is decreased (by separating the water surfaces) equilibrium vapor pressure is established at a supersaturation lower than that indicated by the difference in water surface temperatures. For example, in an atmosphere having approximately 400 nuclei cm^{-3} active at 0.1% supersaturation, we can reduce the amount of available water vapor by increasing the separation between water surfaces so that with the same difference in surface temperature, equilibrium is established by activation of only 50 nuclei cm^{-3}. As these droplets grow and fall out of the chamber the rate at which water is extracted from the environment is decreased, so that equilibrium is established at a slightly higher supersaturation permitting the next most active nuclei to form droplets. The concentration of drops, however, does not increase significantly.

These observations suggest that dense fog might be prevented if extremely hygroscopic, large nuclei are introduced into the atmosphere in small concentrations before the fog begins to form. Using our physical and dynamic models for radiation fog as a basis, conservative calculations indicate that 25 to 50 two-micron diameter lithium chloride particles per cubic centimeter are sufficient to remove the excess water vapor supplied through radiational cooling of the air at 100% relative humidity.

If an equilibrium relative humidity can be maintained at 100% by extraction of water from the atmosphere on the artificial nuclei it seems probable that an effect similar to that observed in the diffusion chamber may result, i.e., the concentration of droplets in the fog may be reduced from the normal 200 cm^{-3} to perhaps 25 to 50 cm^{-3}. With the reduced competition for available water these droplets would grow more rapidly and cause a more favorable drop size distribution.

F. Fog Frequency Distribution in the Continental United States*

During the first year of this project we conducted a brief climatological study of supercooled fogs in the Continental United States and concluded in the First Annual Summary Report No. RM-1788-P-4 that such a fog constituted a significant problem in the pacific northwest but was of only minor concern in other portions of the country. In accordance with plans we have extended the study to include warm fogs by conducting a somewhat detailed study of the distribution of the mean number of days on which heavy fog (visibility of 1/4 mile or less) occurred at 256 reporting stations in the Continental United States. Results of this study are reported here.

Briefly, this survey shows that warm fog is a significant problem at air terminals over 60% of the Continental United States (160 out of 256 stations report heavy fog more than twenty days per year). Fifty of these stations ($\sim$20% of the total) report more than 35 days of heavy fog per year. The mean fog frequency per reporting station in the Continental United States is 27 days per year. These numbers emphasize the severity of the fog problem. The discussion that follows defines the geographical regions of the United States where the fog problem is most severe.

The source of data for this study was the U. S. Department of Commerce, Weather Bureau, Local Climatological data summaries for 256 first order weather stations in the Continental United States. These statistics are based upon the total length of record at each station and represent widely differing numbers of years of observation. Some stations have as few as two years of record, while the frequencies of heavy fog for other stations are based upon as many as sixty to eighty years of observation. Most of the data covers the period through 1963, however many years this may be. A few stations had long records for earlier years, but a change in station location reduced the record to ten years or less in 1963. Earlier data for these stations were acquired and compared with the more current, shorter period statistics.

---

*By Robert L. Peace

By nature, fog is largely a localized weather phenomenon because the causative factors of moisture and cooling are greatly influenced by local terrain and geography. Nevertheless, large geographical areas have sufficiently similar character to allow analysis of fog frequency distribution for intervals of 5 to 10 days/year. Figure 25 is a conventional isopleth analysis of the average annual number of days with heavy fog in the Continental United States. In most areas, local effects appear as random departures from the general pattern.

The fundamental assumption for such an analysis is the continuous distribution of the analyzed parameter. Although this assumption is not completely valid for fog frequency, the analysis demonstrates that it is a reasonable approximation for much of the United States for the data available. The most notable exceptions are the evident discontinuities along the Sierra Nevada Mountains and the central Appalachian Mountains, and the numerous singularities among coastal stations such as New Orleans, La., Point Mugu, Calif., Duluth, Minn. and Nantucket.

The solid isopleths in Figure 25 are drawn for intervals of 10 days. Most of the area east of the Sierra Nevada and Cascade Mountains and west of the Tennessee Valley can be analyzed to twice this detail (dashed 5-day isopleths) without appreciable degeneration of the pattern. On the other hand along the Pacific coast and in the central Appalachians, fog is such a localized phenomenon that with the station density available, even the ten day isopleths cannot be located with any certainty. We therefore sought other means for presenting data.

In the sequence of different types of analyses that were tried, it became evident that the United States could be divided into seven regions (shown in Figure 26) of common terrain and geographic properties that are strongly related to fog frequency. Data were grouped according to these areas and histograms, showing the number of stations reporting heavy fog frequencies within five day frequency intervals, were plotted for each. These histograms and one covering the entire Continental United States are presented in normalized form in Figures 27 through 31. To the extent that the reporting stations

are representative, the figures may be interpreted in terms of the fraction of the total area of the region that is characterized by the fog frequency indicated. A brief discussion of the characteristics that control fog frequency distribution within each region is presented in the text.

Sierra Nevada to the Rocky Mountains

This arid region is cut off from moisture by mountain barriers both east and west. The lack of moisture causes a narrow, uniformly low, fog-frequency distribution. No station in this region averages over 10 days of heavy fog per year, while the majority experience 5 days or less per year.

Great Plains and Mississippi Valley

The uniform terrain and moderate moisture characteristics of this broad region are responsible for the narrow, modest, heavy-fog-frequency distribution displayed in Figure 29a. The principal water source is the Gulf of Mexico but no large water bodies directly influence fog formation in this area. The foothills of the Rocky Mountains tend to broaden the frequency distribution. Five of the seven stations reporting over 20 days of heavy fog per year are located along the eastern slopes of the Rocky Mountains where orographic effects are evident.

Cascade to the Rockey Mountains

This area is characterized by mountains separated by broad, flat valleys. Moisture, though not abundant, is adequately supplied from modest precipitation. As a result, all stations in this region experience an average of at least 11 days of heavy fog per year.

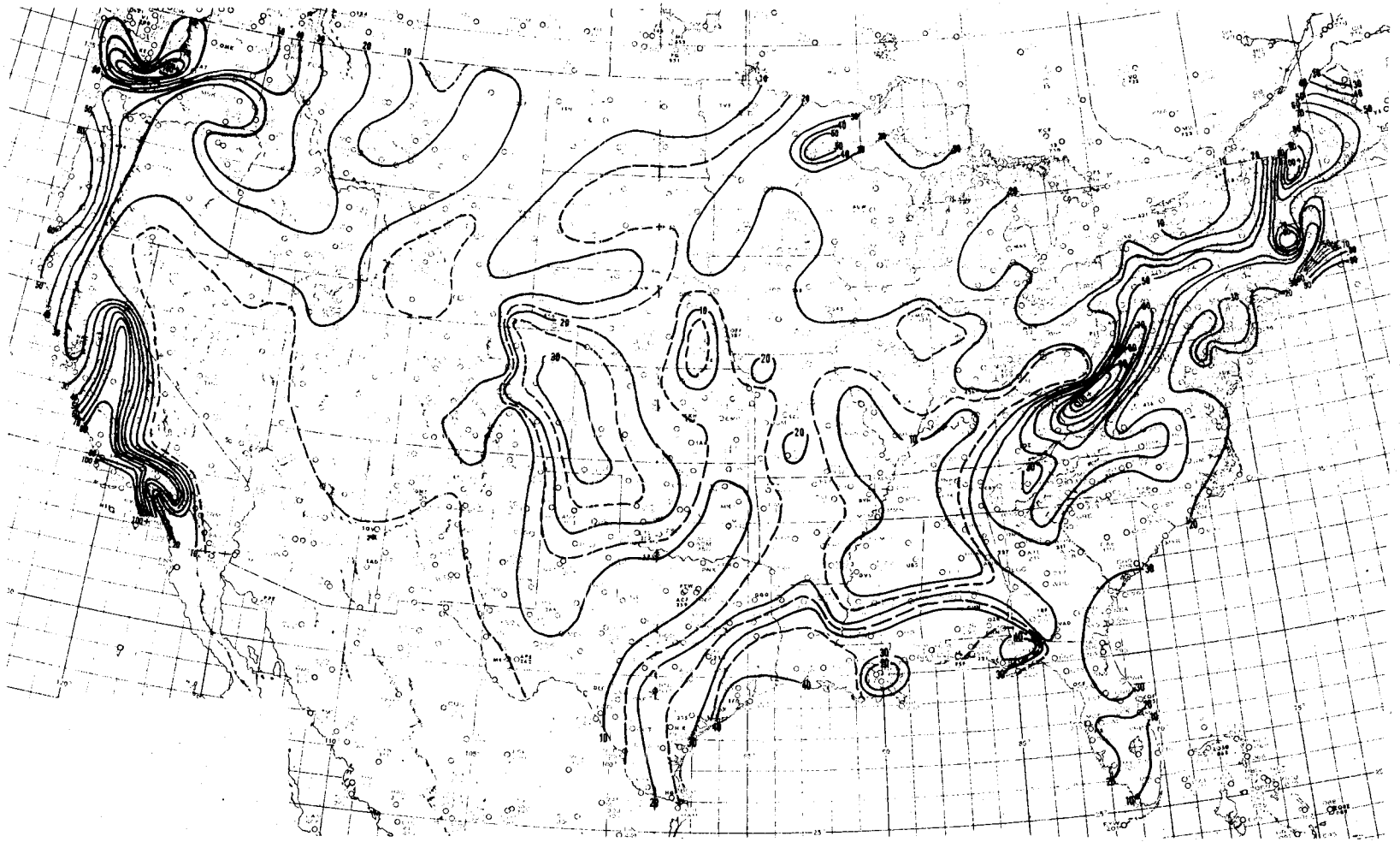

Figure 25 MEAN ANNUAL HEAVY FOG FREQUENCY (DAYS PER YEAR)

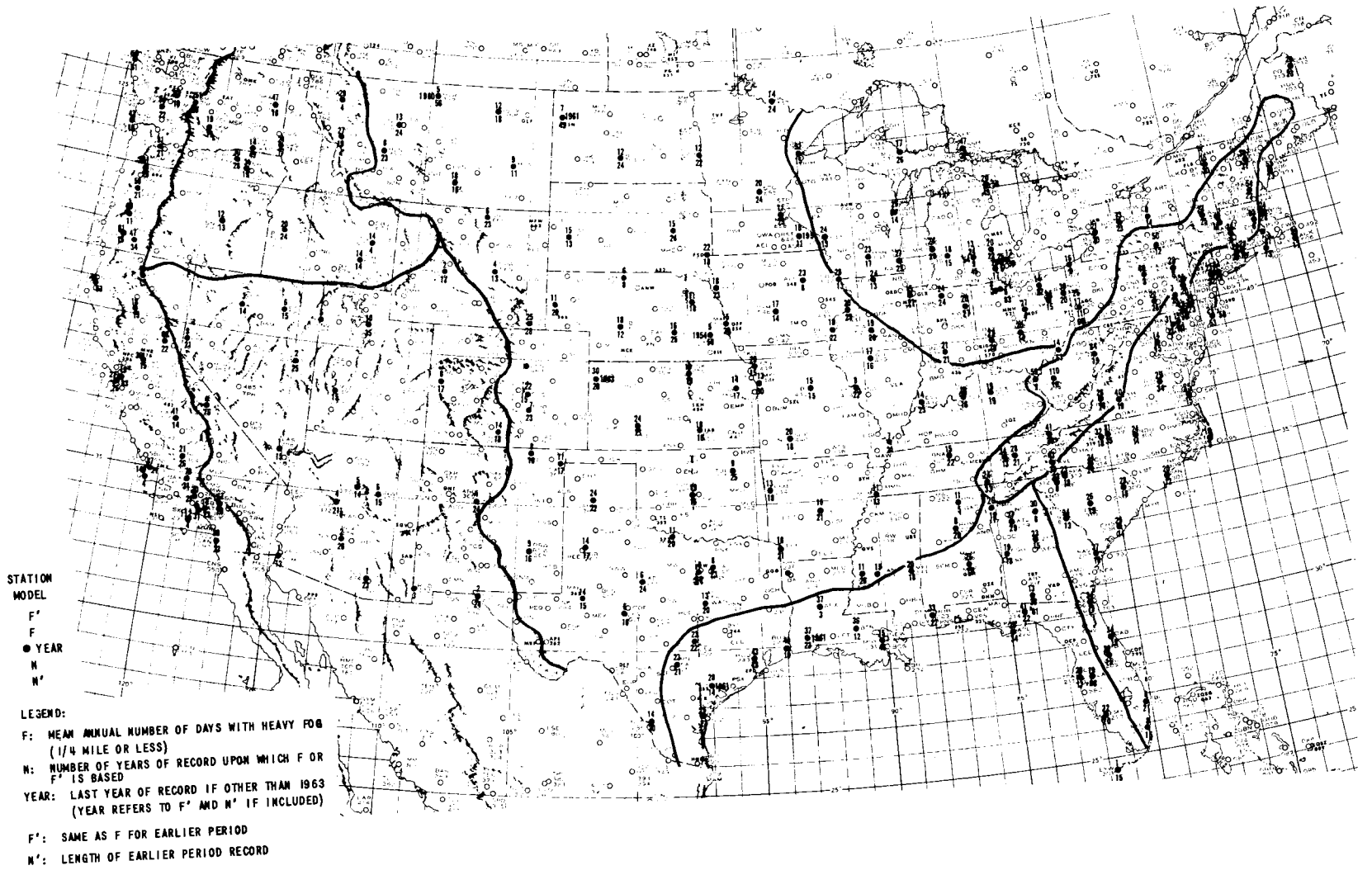

Figure 26 BOUNDARIES OF FOG CLIMATIC REGIONS AND STATION FREQUENCY DATA

Great Lakes Area

The influence of the Great Lakes extends south of the lakes to an ill-defined border with the Great Plains and Mississippi Valley region. To the east, the Appalachians form a more distinct border of the Great Lakes area. Heavy fog is understandably higher near the Great Lakes than in the Great Plains. The spread of fog frequencies is also greater in this area. The highest fog frequencies are near the water, but fog frequency does not vary as much with distance from the water as it does between stations at comparable distances from water.

West Coast

The area west of the Sierra Nevada and Cascade Mountains is under the influence of the Pacific Ocean and the orographic lift provided by the mountains. As a consequence, heavy fog frequency is generally high. The irregular terrain and varying proximity of reporting stations to the ocean, causes a wide spread in heavy fog frequencies. The greatest frequencies occur along the shore of southern California and at the stations located high in the mountains, particularly in northern California and Oregon.

Appalachian Mountains

The Appalachian Mountains region resembles the West Coast region in many ways. Both are areas of irregular terrain and substantial moisture, with orographic lift of west to east flow. As a result, the fog frequency distributions in the two regions are very similar, both showing high average incidence and large frequency spread. The annual number of days with heavy fog in the Appalachians varies from a low of 22 days to a high of 307 days. In general, the greatest fog frequency is found to the west of the highest terrain due to orographic lift of the predominant westerly winds.

Atlantic and Gulf Coasts

These two coastal regions were at first treated separately, but because of the strong similarity of their respective fog-frequency distributions they have been combined into a single region. Both coasts display a moderately broad frequency distribution around a relatively high model frequency. However, despite the proximity of large bodies of water the frequency spread is substantially less than that of either the Appalachian Mountain region or the west coast areas -- where irregular terrain creates widely diverse local fog-producing conditions. The one extreme local influence in this area is found in the Nantucket and Block Island area where the heavy fog frequency is about twice that of the other stations along these coasts.

Local environment differences are not the only explanation for the apparent discrepancies between adjacent stations. Both long and short-term mean annual heavy fog-frequency statistics were acquired for fourteen stations whose 1963 means were based upon ten years of record or less. In most instances where such a double record was acquired, the long period statistics indicate fewer days with heavy fog than do those of the shorter period. The following is a comparison between long and short-term mean annual number of days with heavy fog for the fourteen stations for which such data are available.

Tallahassee, Florida	55 days/yr.	for 2 yrs.	41 days/yr.	for 22 yrs.
Lake Charles, Louisiana	51	2	37	23
Lansing, Michigan	24	9	13	45
Rochester, Minnesota	38	3	16	11
Saint Louis, Missouri	10	6	8	22
Lincoln, Nebraska	7	8	5	58
Atlantic City, New Jersey	43	5	21	53
Williston, North Dakota	9	2	7	45
Toledo, Ohio	20	8	8	83
Fort Worth, Texas	10	10	8	55

Alpena, Michigan	18	4	20	45
Glasgow, Montana	11	8	12	18
Havre, Montana	5	3	5	56
Victoria, Texas	24	2	28	14

Although there are several possible explanationsfor these differences between long and short-term means -- change in observing procedure, climatic change, increased idustrialization, poor choice of airport or observation sites, etc. -- the available data are not sufficient to ascertain the actual cause. The mere existance of this discrepancy, coupled with the wide variation in length of record for the 256 stations used in the analysis does, however, suggest that length of record may contribute to the variation between stations in a given area.

Separation of this effect and that of local environmental conditions is difficult or impossible where two stations in close proximity have both substantially different lengths of record and reported fog frequency. Detroit, Michigan is one example of this problem. Only twenty miles separates two stations having 5 and 30 years of record and mean annual heavy fog frequencies of 25 and 12 days respectively.

Despite the difficulties imposed by the type of data available and the largely local nature of fog, the analysis provides significant insight into the nationwide climatology of fog. The differences in mean and modal frequency of heavy fog and the differences in the degree of local influence from region to region are real and quite pronounced. It is obvious that heavy fog is not a problem in the southwestern mountain region and only a moderate problem in the Great Plains. On the other hand, fog is most frequent and quite local in nature along the West Coast, in the Appalachian Mountains and along the New England Coast. Along the Gulf and Atlantic Coasts and in the Great Lakes region fog is quite frequent (more than 20 days per year on the average) and local effects do not seem to be as significant as in other areas of high incidence.

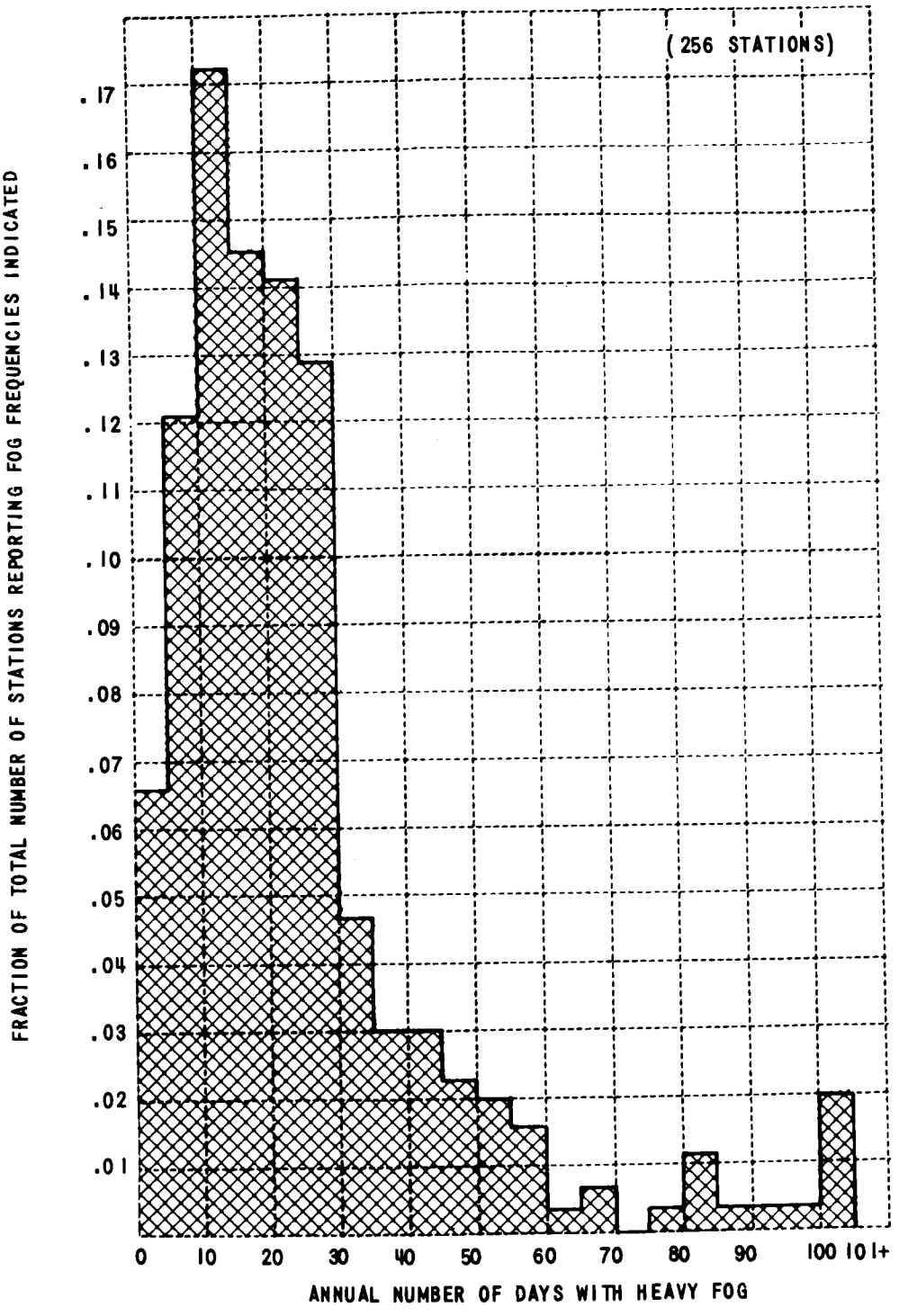

Figure 27

FOG FREQUENCY HISTOGRAM - ENTIRE UNITED STATES

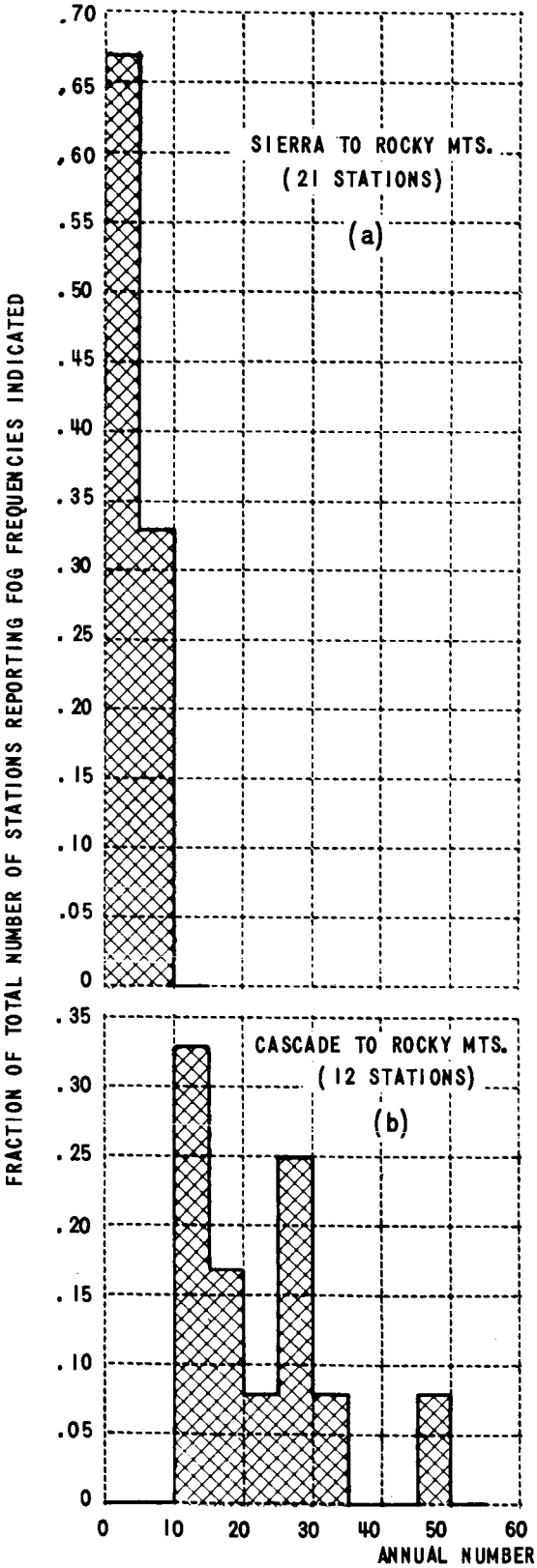

Figure 28

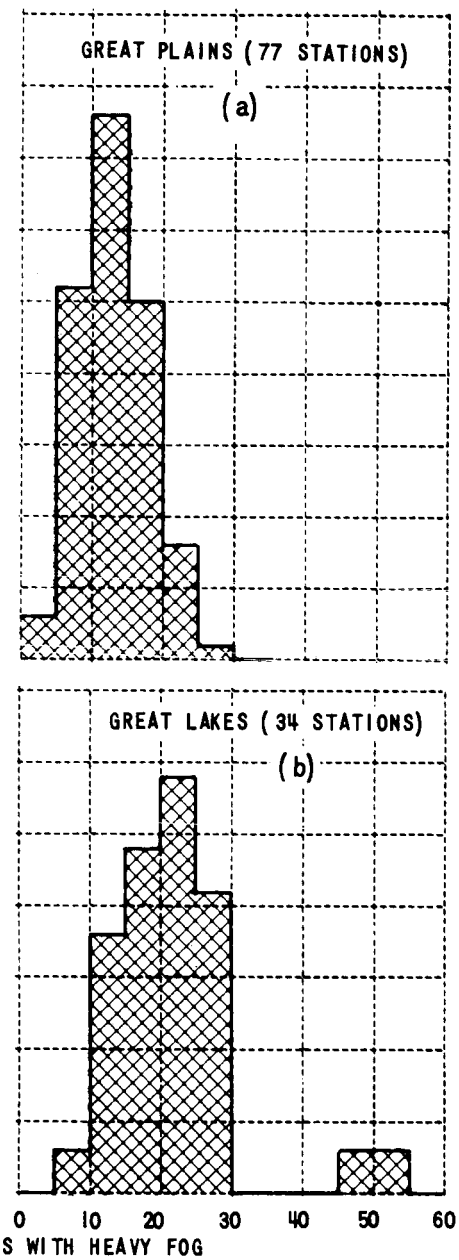

Figure 29

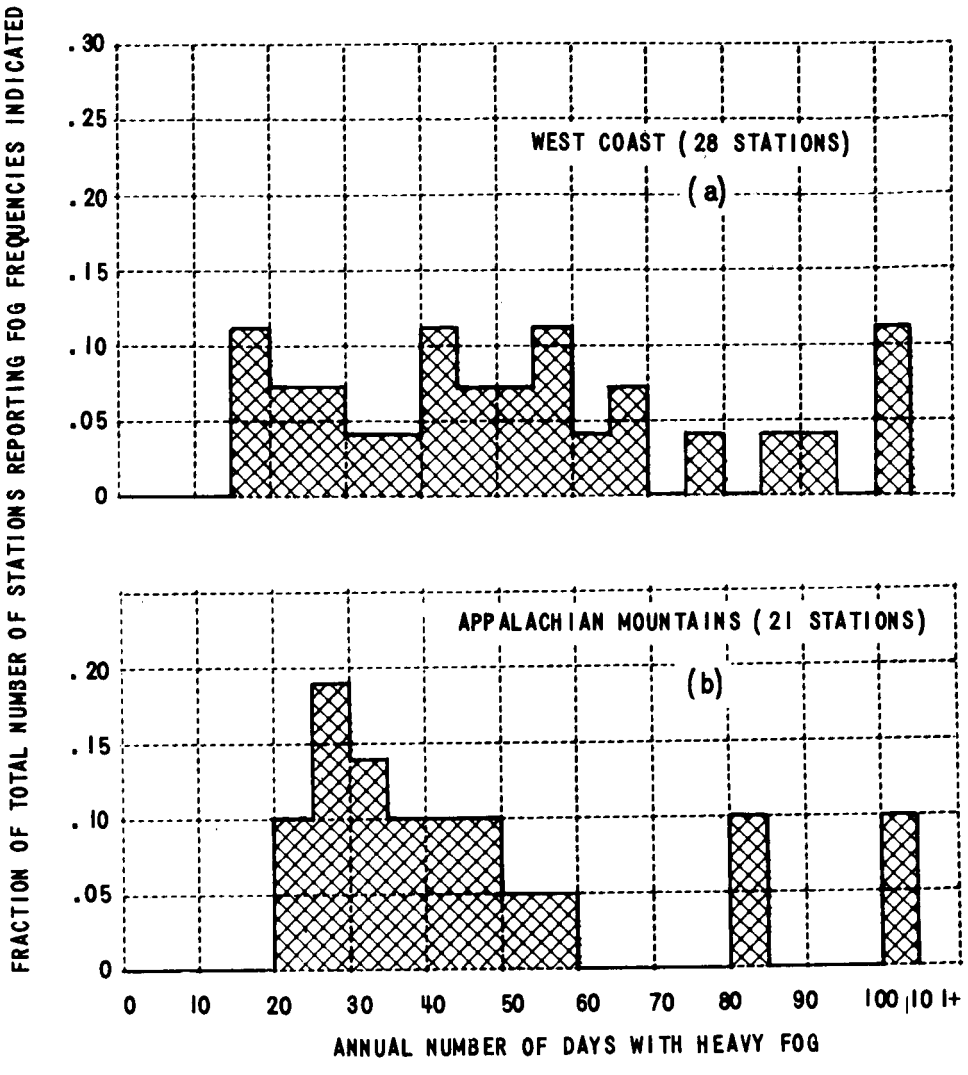
FRACTION OF TOTAL NUMBER OF STATIONS REPORTING FOG FREQUENCIES INDICATED
.30
.25
.20
.15
.10
.05
0
WEST COAST (28 STATIONS)
(a)
APPALACHIAN MOUNTAINS (21 STATIONS)
(b)
0
10
20
30
40
50
60
70
80
90
100
101+
ANNUAL NUMBER OF DAYS WITH HEAVY FOG

Figure 30

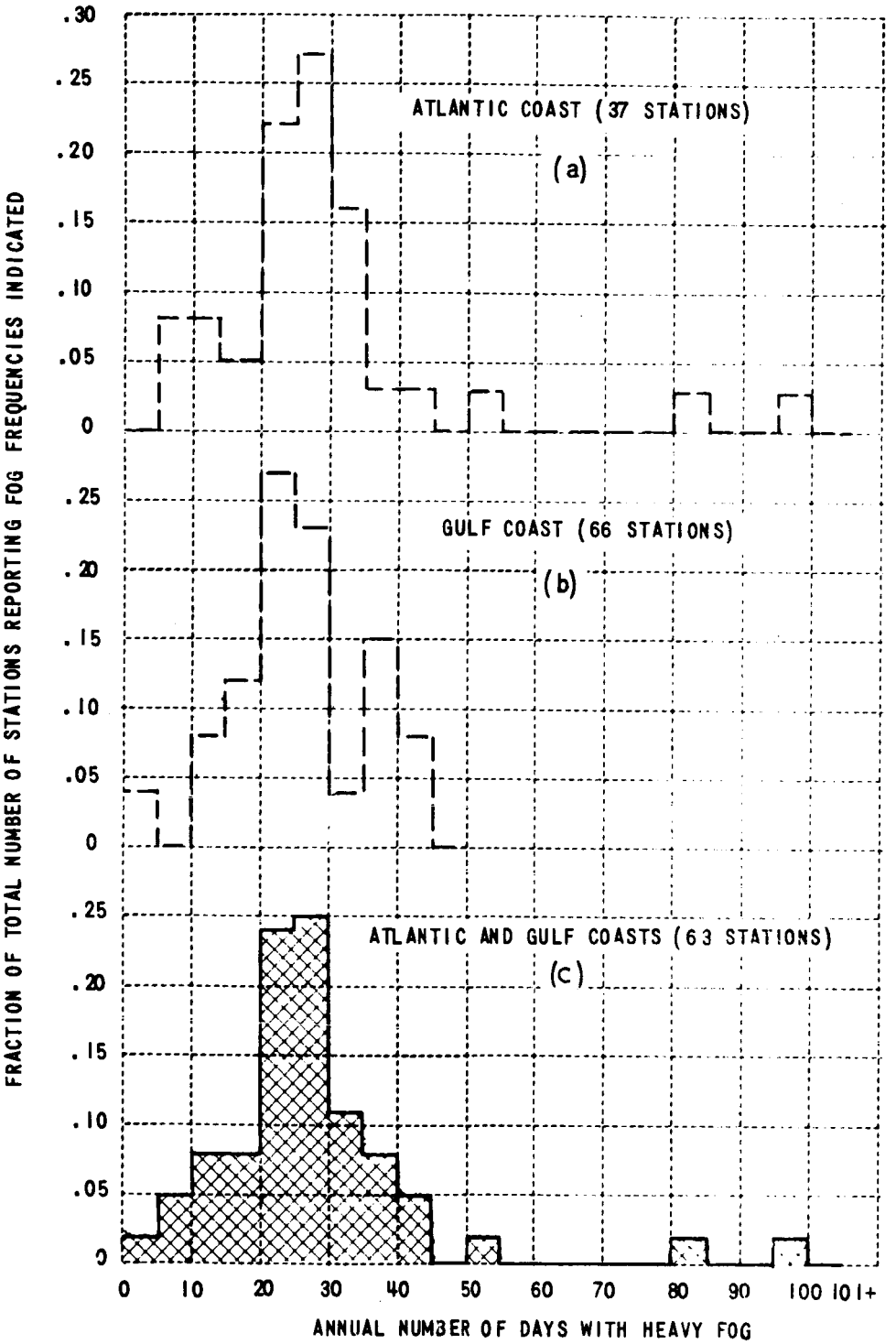
FRACTION OF TOTAL NUMBER OF STATIONS REPORTING FOG FREQUENCIES INDICATED
.30
.25
.20
.15
.10
.05
0
ATLANTIC COAST (37 STATIONS)
(a)
GULF COAST (66 STATIONS)
(b)
ATLANTIC AND GULF COASTS (63 STATIONS)
(c)
0 10 20 30 40 50 60 70 80 90 100 101+
ANNUAL NUMBER OF DAYS WITH HEAVY FOG

Figure 31

REFERENCES

aufm Kampe, H. K., J. J. Kelly, and H. K. Weickmann, 1957: Seeding Experiments in Subcooled Stratus Clouds, Cloud and Weather Modification, Amer. Meteor. Soc., Boston.

Benton, D. P., G. A. Elton, E. A. Peace, and R. G. Picnett, 1958: Coalescence of Droplets in Aqueous Disperse Aerosols, Int. J. Air Pollution, Pergamon Press, 1, 44.

Brunt, D., 1935: Condensation By Mixing, Quart. J. Roy. Met. Soc., 61, 213.

Cobine, J. D., 1958: Gaseous Conductors, Dover Publications, Inc., New York, 252-258.

Cochet, R., 1951: Evolution dúne gouttelette déau chargée dans un novage ou un brouillardá temperature positive, C. R. Acad. Sci., Paris, 233, 190.

Elton, G. A., 1953: A Possible Method of Fog Dispersal, Chemistry and Industry, (7 March), 219.

Jiusto, J. E., 1964: Project FOG DROPS, First Annual Summary Report, Cornell Aeronautical Laboratory, Inc., Report No. RM-1788-P-4.

Jiusto, J. E. and R. J. Pilié, 1958: Condensation Nuclei Experiments with Simple Apparatus, Weatherwise, Vol. II, No. 6.

Jiusto, J. E. and R. R. Rogers, 1960: Greenland Whiteout Experiments - Summer 1960, Summary Report, Cornell Aeronautical Laboratory, Inc., Report No. RM-1430-P-2.

Lieberman, A., 1960: Warm Fog and Cloud Dissipation, Armour Research Foundation, Chicago, Ill., ARF-3153-6, Air Force Cambridge Res. Lab., Report 260.

Lumley, J. L. and H. A. Panofsky, 1964: The Structure of Atmospheric Turbulence, John Wiley and Sons, New York, 239 pgs.

Mason, B. J., 1957: The Physics of Clouds, Oxford University Press.

Mason, B. J., O. W. Jayaratne, J. D. Woods, 1963: An Improved Vibrating Capillary Device for Producing Uniform Water Droplets of 15 to 500μm Radius, Jour. Sci. Inst., Vol. 40, 247.

McVehil, G. E., 1964: Wind and Temperature Profiles Near the Ground in Stable Stratification. Quart. Journ. Roy. Met. Soc., 90, 384.

Monin, A. S., and A. M. Obukhov, 1954: Basic Laws of Turbulent Mixing in the Ground Layer of the Atmosphere. Akad. Nauk., S.S.S.R., Geophys. Inst. Trudy, No. 24 (151), 163.

Panofsky, H. A., A. K. Blackadar, and G. E. McVehil, 1960: The Diabatic Wind Profile. Quart. Journ. Roy. Met. Soc., 86, 390.

Pauthenier, M., 1947: Sur le balayage des bruillards, C. R. Acad. Sci., Paris, 224, 142.

Rodhe, B., 1962: The Effect of Turbulence on Fog Formation, Tellus, 14, 49.

Sartor, J. D., 1960a: The Role of Electrostatic Field in the Coagulation of Fog and Cloud Droplets, P-2134, The Rand Corporation, Santa Monica, California.

Schaefer, V. J., 1946: The Production of Ice Crystals in a Cloud of Supercooled Water Droplets, Science, 104.

Schulepov, Yu. V., and S. S. Dukhin, 1962: In Reference to the Theory of Electrical Coagulation of Spherical Aerosol Particles, Kolloidnyy Zhurnal 24, 6, 749 (Translation appears in AF, Foreign Technology Division, Rept. M.T.-63-70 (July 17, 1963.)).

Taylor, G. I., 1917: The Formation of Fog and Mist, Quart. Jour. Roy. Met. Soc., 43, 241.

Twomey, S., 1959: The Nuclei of Natural Cloud Formation - Part I, Geof. Pura. E. Appl. - Milano, 43, 227.

Vonnegut, B., and C. B. Moore, 1958: Preliminary Attempts to Influence Convective Electrification in Cumulus Clouds by the Introduction of Space Charge into the Lower Atmosphere. Conf. on Atmos. Elect., Wentworth-by-the-sea, N. H., A. D. Little, Inc., Cambridge, Mass.